

# Dilute Multi Alpha Cluster States in Nuclei

Taiichi Yamada

*Laboratory of Physics, Kanto Gakuin University, Yokohama 236-8501, Japan and  
Institute de Physique Nucléaire, F-91406 Orsay Cedex, France*

Peter Schuck

*Institute de Physique Nucléaire, F-91406 Orsay Cedex, France*

(Dated: November 9, 2018)

## Abstract

Dilute multi  $\alpha$  cluster condensed states with spherical and axially deformed shapes are studied with the Gross-Pitaevskii equation and Hill-Wheeler equation, where the  $\alpha$  cluster is treated as a structureless boson. Applications to self-conjugate  $4N$  nuclei show that the dilute  $N\alpha$  states of  $^{12}\text{C}$  to  $^{40}\text{Ca}$  with  $J^\pi = 0^+$  appear in the energy region from threshold up to about 20 MeV, and the critical number of  $\alpha$  bosons that the dilute  $N\alpha$  system can sustain as a self-bound nucleus is estimated roughly to be  $N_{cr} \sim 10$ . We discuss the characteristics of the dilute  $N\alpha$  states with emphasis on the  $N$  dependence of their energies and rms radii.

PACS numbers: 21.10.Dr, 21.10.Gv, 03.75.Hh

## I. INTRODUCTION

The molecular-like picture as well as the single-particle picture are fundamental viewpoints to understand the structure of light nuclei.[1, 2, 3, 4] It is well known that the structure of many states in light nuclei is described successfully by the microscopic cluster model, where a group of nucleons is assumed to form a localized substructure (cluster), interacting with other clusters and/or nucleons in the nucleus. The predominant cluster is the  $\alpha$  nucleus, which plays an important role in the cluster model, because it is the lightest and also smallest shell-closed nucleus with a binding energy as large as 28 MeV, reflecting the strong four-nucleon correlation. Molecular-like states in nuclei are expected to appear around the threshold energy of breakup into constituent clusters [5], because the intercluster binding is weak in the cluster states. For example, the ground state of  ${}^8\text{Be}$  and the second  $0^+$  state of  ${}^{12}\text{C}$  are known [6] to have loosely bound  $2\alpha$  and  $3\alpha$  structures, respectively, which appear around the  $2\alpha$  and  $3\alpha$  thresholds.

Special attention has been paid to such four-nucleon correlations corresponding to an  $\alpha$ -type condensation in symmetric nuclear matter, similar to the Bose-Einstein condensation for finite number of dilute bosonic atoms such as  ${}^{87}\text{Rb}$  or  ${}^{23}\text{Na}$  at very low temperature [7]. Several authors have discussed the possibility of  $\alpha$ -particle condensation in low-density nuclear matter [8, 9]. They found that such  $\alpha$  condensation can occur in the low-density region below a fifth of the saturation density, although the ordinary pairing correlation can prevail at higher density. The result indicates that  $\alpha$  condensate states in finite nuclear system may exist in excited states of dilute density composed of weakly interacting gas of  $\alpha$  particles. Thus, it is an interesting subject to study the structure of light nuclei from the viewpoint of  $\alpha$ -particle condensation.

Recently, a new  $\alpha$ -cluster wave function was proposed which is of the  $N\alpha$ -particle condensate type [10]:

$$|\Phi_{N\alpha}\rangle = (C_\alpha^+)^N |\text{vac}\rangle, \quad (1)$$

$$\langle \mathbf{r}_1 \cdots \mathbf{r}_N | \Phi_{N\alpha} \rangle \propto \mathcal{A} \left\{ e^{-\nu(\mathbf{r}_1^2 + \cdots + \mathbf{r}_N^2)} \phi(\alpha_1) \cdots \phi(\alpha_N) \right\}, \quad (2)$$

where  $C_\alpha^+$  is the  $\alpha$ -particle creation operator,  $\phi(\alpha)$  denotes the internal wave function of the  $\alpha$  cluster,  $\mathbf{r}_i$  is the center-of-mass coordinate of the  $i$ -th  $\alpha$  cluster, and  $\mathcal{A}$  presents the antisymmetrization operator among the constituent nucleons. The important characteristic

in Eq. (2) is that the center-of-mass motion of each  $\alpha$  cluster is of  $S$ -wave type with the independent size parameter  $\nu$ . Applications of the condensate-type wave function to  $^{12}\text{C}$  and  $^{16}\text{O}$  showed that the second  $0^+$  state of  $^{12}\text{C}$  ( $E_x=7.65$  MeV) and fifth  $0^+$  states of  $^{16}\text{O}$  ( $E_x=14.0$  MeV), located around the  $3\alpha$ - and  $4\alpha$ -particle thresholds, respectively, are specified by the  $N\alpha$  condensate state, which is quite similar to the Bose-Einstein condensation of bosonic atoms in magnetic traps where all atoms occupy the lowest  $S$ -orbit.[10] The calculated root-mean-square (rms) radius for those condensate states is about 4 fm, which is much much larger than that for the ground state (about 2.7 fm). As for  $^8\text{Be}$ , the  $\alpha$ -particle wave function in Eqs. (1) and (2), taking into account the axially symmetric deformation, was applied to investigate the rotational structure of the ground-band states ( $0^+-2^+-4^+$ ) [11]. It was found that the rotational character of the  $^8\text{Be}$  ground state band is reproduced nicely by this wave function with deformation [11].

The above-mentioned theoretical results for  $^8\text{Be}$ ,  $^{12}\text{C}$  and  $^{16}\text{O}$  lead us to conjecture that such dilute  $\alpha$ -cluster states near the  $N\alpha$  threshold may also occur in other heavier  $4N$  self-conjugate nuclei. The Coulomb potential barrier should play an important role to confine such dilute  $N\alpha$ -particle states, as inferred from the analyses of the  $^8\text{Be}$ ,  $^{12}\text{C}$  and  $^{16}\text{O}$  nuclei. In fact, the ground state of  $^8\text{Be}$ , which appears at  $E_{2\alpha} = 92$  keV referring to the  $2\alpha$  threshold, exists as a resonant state with very narrow width, due to the Coulomb potential barrier, whose height is estimated to be  $1 \sim 2$  MeV. This self-trapping of  $\alpha$ -particles by the Coulomb barriers is in contrast to the case of the dilute neutral atomic condensate states, where the atoms are trapped by the external magnetic field [7].

It is an intriguing problem and of interest to study how many  $\alpha$  particles can be bound in the dilute nuclear system. Increasing the number of  $\alpha$  clusters, the rms radius of the system should become gradually larger, because the dilute character must be retained. Then, the total kinetic energy of the  $N\alpha$  system becomes significantly smaller in comparison with the potential energy, similar to the case of bosonic atoms in the condensed state. In addition, the height of the Coulomb potential barrier will become steadily lower. This is due to the following reasons. The  $\alpha$ - $\alpha$  nuclear potential is short-ranged, while the Coulomb potential is long-ranged. Increasing the number of the  $\alpha$  particles, the repulsive contribution from the Coulomb potentials prevails gradually over the attractive one from the  $\alpha$ - $\alpha$  nuclear potentials, because the gas-like  $N\alpha$  system is expanding in such a way that the rms radius between two  $\alpha$  particles is gradually getting larger. This means that the height of the

potential barrier confining the gas-like  $N\alpha$  particles becomes lower with increasing  $N$ , and then, there should exist a critical number ( $N = N_{cr}$ ) beyond which the  $N\alpha$  system can not sustain itself as a bound nuclear state. Thus, it is interesting to estimate the number of  $N_{cr}$  as well as to study the structure of the dilute  $N\alpha$  system up to  $N = N_{cr}$ . Since the application of the condensate-type wave function in Eqs. (1) and (2) to the general  $N\alpha$  system is not easy and the computational limitation is  $N \sim 6$  at most, we need to study them with phenomenological models.

In this paper, the gas-like  $N\alpha$  cluster states are studied with the following two approaches: the Gross-Pitaevskii-equation approach and Hill-Wheeler-equation approach. The Gross-Pitaevskii equation, which is of the nonlinear-Schrödinger-type, was proposed about fifty years ago to describe the single-boson motion in the dilute atomic condensate state [12]. Recent experiments starting from the middle of 1990's have succeeded in realizing such a condensate state consisting of  $10^5$ - $10^6$  neutral atoms trapped by the magnetic field at very low temperature. Many characteristic aspects of the dilute states are described successfully by the Gross-Pitaevskii equation [7]. Thus, its application to the dilute  $N\alpha$  nuclear systems is also very promising, and we expect from such a study useful information on the condensed states. On the other hand, we here propose also a different approach. Although the Gross-Pitaevskii equation is simple and interesting for the study of the structure of the dilute  $N\alpha$  system, the center-of-mass motion in the  $N\alpha$  system is not completely removed in this framework. The effect of the center-of-mass motion should be non-negligible to the total energy and rms radius etc. for small numbers of  $\alpha$  bosons. We, thus, formulate in this paper the framework describing the dilute  $N\alpha$  systems free from the center-of-mass motion, with the approach of the Hill-Wheeler equation. The spherical  $N\alpha$  systems as well as the deformed ones, with the axial symmetry, are discussed with this equation. The two different approaches, the Gross-Pitaevskii-equation approach and the Hill-Wheeler-equation approach, are complementary to one another, and we will obtain useful understanding of the dilute multi  $\alpha$ -particle states. Starting from  ${}^8\text{Be}$ , the structure of the gas-like  $N\alpha$  boson systems with  $J^\pi = 0^+$  is investigated and the critical number  $N_{cr}$  is estimated with those two different approaches.

The paper is organized as follows. We formulate in Sec. II the Gross-Pitaevskii-equation approach and the Hill-Wheeler-equation approach for the dilute  $N\alpha$  system. In Sec. III the calculated results are presented, and the characteristics of the dilute  $N\alpha$  states are discussed

with emphasize on the  $N$  dependence of their energies and rms radii. A summary finally is given in Sec. IV.

## II. FORMULATION

In this section, we formulate the two approaches to study the structure of the dilute  $N\alpha$  nuclear systems: the Gross-Pitaevskii-equation approach and Hill-Wheeler-equation approach.

### A. Gross-Pitaevskii equation for dilute $N\alpha$ nuclear systems

In the mean field approach, the total wave function of the condensate  $N\alpha$ -boson system is represented as

$$\Phi(N\alpha) = \prod_{i=1}^N \varphi(\mathbf{r}_i), \quad (3)$$

where  $\varphi$  and  $\mathbf{r}_i$  are the normalized single- $\alpha$  wave function and coordinate of the  $i$ -th  $\alpha$  boson. Then, the equation of motion for the  $\alpha$  boson, called as the Gross-Pitavskii equation, is of non-linear Schrödinger-type,

$$-\frac{\hbar^2}{2m} \left(1 - \frac{1}{N}\right) \nabla^2 \varphi(\mathbf{r}) + U(\mathbf{r})\varphi(\mathbf{r}) = \varepsilon \varphi(\mathbf{r}), \quad (4)$$

$$U(\mathbf{r}) = (N-1) \int d\mathbf{r}' |\varphi(\mathbf{r}')|^2 v_2(\mathbf{r}', \mathbf{r}) + \frac{1}{2}(N-1)(N-2) \int d\mathbf{r}'' d\mathbf{r}' |\varphi(\mathbf{r}'')|^2 |\varphi(\mathbf{r}')|^2 v_3(\mathbf{r}'', \mathbf{r}', \mathbf{r}), \quad (5)$$

where  $m$  stands for the mass of the  $\alpha$  particle,  $U$  is the mean-field potential of  $\alpha$ -particles, and  $v_2$  ( $v_3$ ) denotes the  $2\alpha$  ( $3\alpha$ ) interaction. The center-of-mass kinetic energy correction,  $1 - 1/N$ , is taken into account together with the finite number corrections,  $N - 1$ , etc. In the present study, only the  $S$ -wave state is solved self-consistently with the iterative method. The total energy of the  $N\alpha$  system  $E(N\alpha)$  is presented as

$$E(N\alpha) = N \left[ \langle t \rangle + \frac{1}{2}(N-1)\langle v_2 \rangle + \frac{1}{6}(N-1)(N-2)\langle v_3 \rangle \right], \quad (6)$$

$$\langle t \rangle = \left(1 - \frac{1}{N}\right) \times \langle \varphi(\mathbf{r}) | -\frac{\hbar^2}{2m} \nabla^2 | \varphi(\mathbf{r}) \rangle, \quad (7)$$

$$\langle v_2 \rangle = \langle \varphi(\mathbf{r}) \varphi(\mathbf{r}') | v_2(\mathbf{r}, \mathbf{r}') | \varphi(\mathbf{r}) \varphi(\mathbf{r}') \rangle, \quad (8)$$

$$\langle v_3 \rangle = \langle \varphi(\mathbf{r}) \varphi(\mathbf{r}') \varphi(\mathbf{r}'') | v_3(\mathbf{r}, \mathbf{r}', \mathbf{r}'') | \varphi(\mathbf{r}) \varphi(\mathbf{r}') \varphi(\mathbf{r}'') \rangle, \quad (9)$$

and the eigen energy  $\varepsilon$  in Eq. (4) is given as

$$\varepsilon = \langle t \rangle + (N - 1)\langle v_2 \rangle + \frac{1}{2}(N - 1)(N - 2)\langle v_3 \rangle. \quad (10)$$

The nuclear rms radius in the  $N\alpha$  state is evaluated as,

$$\sqrt{\langle r_N^2 \rangle} = \sqrt{\langle r_\alpha^2 \rangle_{GP} + 1.71^2}, \quad (11)$$

$$\langle r_\alpha^2 \rangle_{GP} = \left(1 - \frac{1}{N}\right) \langle \varphi | r^2 | \varphi \rangle, \quad (12)$$

where we take into account the finite size effect of the  $\alpha$  particle and the correction of the center-of-mass motion.

## B. Hill-Wheeler equation for dilute $N\alpha$ states

The framework of the Gross-Pitaevskii approach is simple and useful for the study of the structure of the dilute  $N\alpha$  systems. The center-of-mass motion, however, is not removed exactly in this approach. The effect on the total energy and rms radius etc. is not negligible for the small-number  $\alpha$ -boson systems. We formulate here the Hill-Wheeler-equation approach for the axially symmetric  $N\alpha$  systems as well as for the spherical ones, in which the center-of-mass motion is completely eliminated. Only the Hill-Wheeler equation for the deformed  $N\alpha$  systems with the axial symmetry is provided in this section, because the limit of the spherical systems is included in the deformed case.

The single  $\alpha$ -particle wave function should be mainly in the lowest  $S$  state in the gas-like  $N\alpha$  boson system. Thus, the model wave function of the axially symmetric  $N\alpha$  system should be described in terms of a superposition of a Gaussian basis with axially symmetric deformation (taking the  $z$ -axis as the symmetric axis) as follows,

$$\Phi^{(int)}(N\alpha) = \sum_{\nu_1, \nu_3} f(\nu_1, \nu_3) \Phi^{(int)}(\nu_1, \nu_3), \quad (13)$$

$$\Phi^{(int)}(\nu_1, \nu_3) = \int d\mathbf{R}_{cm} \Phi^{(cm)*}(\mathbf{R}_{cm}; \nu_1, \nu_3) \Phi(\nu_1, \nu_3), \quad (14)$$

$$\Phi(\nu_1, \nu_3) = \prod_{i=1}^N \phi(\mathbf{r}_i; \nu_1, \nu_3) = \Phi^{(int)}(\nu_1, \nu_3) \Phi^{(cm)}(\mathbf{R}_{cm}; \nu_1, \nu_3), \quad (15)$$

$$\phi(\mathbf{r}; \nu_1, \nu_3) = \left(\frac{2\pi}{\nu_1}\right)^{\frac{1}{2}} \left(\frac{2\pi}{\nu_3}\right)^{\frac{1}{4}} \exp\left(-\nu_1 x^2 - \nu_1 y^2 - \nu_3 z^2\right), \quad (16)$$

$$\Phi^{(cm)}(\mathbf{R}_{cm}; \nu_1, \nu_3) = \phi(\mathbf{R}_{cm}; N\nu_1, N\nu_3), \quad (17)$$

where  $\mathbf{r}_i$  ( $\mathbf{R}_{cm}$ ) denotes the coordinate of the  $i$ -th  $\alpha$  boson (the center-of-mass coordinate of the  $N\alpha$  system), and  $\nu_1$  ( $\nu_3$ ) presents the Gaussian size parameter of the  $x$  and  $y$  directions ( $z$ ). The wave function in Eq. (13) is totally symmetric under any exchange of two  $\alpha$  bosons. The angular-momentum-projected total wave function for dilute  $N\alpha$  systems free from the center-of-mass motion is given as

$$\Phi_{JM}^{(int)}(N\alpha) = \sum_{\nu_1, \nu_3} f_J(\nu_1, \nu_3) \Phi_{JM}^{(int)}(\nu_1, \nu_3), \quad (18)$$

$$\Phi_{JM}^{(int)}(\nu_1, \nu_3) = \int d\cos\theta d_{M0}^J(\theta) \mathcal{R}_y(\theta) \Phi^{(int)}(\nu_1, \nu_3), \quad (19)$$

where  $\mathcal{R}_y$  denotes the rotation operator around the  $y$  axis. Setting  $\nu_3 = \nu_1$  in Eq. (18), we obtain the wave function for the spherical  $N\alpha$  system, where only  $J^\pi = 0^+$  state is allowed. The matrix element of a translational invariant scalar operator  $\hat{O}$  with respect to the angular momentum projected  $N\alpha$  wave function in Eq. (19) is evaluated as

$$\begin{aligned} & \langle \Phi_{JM=0}^{(int)}(\nu_1, \nu_3) | \hat{O} | \Phi_{JM=0}^{(int)}(\nu_1', \nu_3') \rangle \\ &= \int d\cos\theta d_{00}^J(\theta) \langle \Phi^{(int)}(\nu_1, \nu_3) | \mathcal{R}_y(\theta) \hat{O} | \Phi^{(int)}(\nu_1', \nu_3') \rangle, \end{aligned} \quad (20)$$

$$= \int d\cos\theta d_{00}^J(\theta) \frac{\langle \Phi(\nu_1, \nu_3) | \mathcal{R}_y(\theta) \hat{O} | \Phi(\nu_1', \nu_3') \rangle}{\langle \Phi^{(cm)}(\mathbf{R}_{cm}; \nu_1, \nu_3) | \mathcal{R}_y(\theta) | \Phi^{(cm)}(\mathbf{R}_{cm}; \nu_1', \nu_3') \rangle}, \quad (21)$$

The total Hamiltonian of the  $N\alpha$ -boson system is given as

$$\mathcal{H} = \sum_{i=1}^N t_i - T_{cm} + \sum_{i<j} v_2(\mathbf{r}_i, \mathbf{r}_j) + \sum_{i<j<k} v_3(\mathbf{r}_i, \mathbf{r}_j, \mathbf{r}_k), \quad (22)$$

where  $v_2$  and  $v_3$  denotes, respectively, the  $2\alpha$  and  $3\alpha$  interactions. The kinetic energy of the center-of-mass motion ( $T_{cm}$ ) is subtracted from the Hamiltonian.

The equation of motion for the dilute  $N\alpha$ -boson states are given in terms of the Hill-Wheeler equation [13]:

$$\sum_{\nu_1', \nu_3'} \left\{ \langle \Phi_J^{(int)}(\nu_1, \nu_3) | \mathcal{H} - E | \Phi_J^{(int)}(\nu_1', \nu_3') \rangle \right\} f_J(\nu_1', \nu_3') = 0, \quad (23)$$

where  $\mathcal{H}$  is the total Hamiltonian of the  $N\alpha$ -boson system in Eq. (22). The coefficients  $f_J$  and eigen energies  $E$  are obtained by solving the Hill-Wheeler equation. In the numerical calculation, the Gaussian size parameters  $\nu_1$  and  $\nu_3$  are discretized and chosen to be of geometric progression,

$$\nu_1^{(k)} = \left(1/b_1^{(k)}\right)^2, \quad b_1^{(k)} = b_1^{(1)} r_1^{k-1}, \quad k = 1 \sim k_{max}, \quad (24)$$

$$\nu_3^{(K)} = \left(1/b_3^{(K)}\right)^2, \quad b_3^{(K)} = b_3^{(1)} r_3^{K-1}, \quad K = 1 \sim K_{max}, \quad (25)$$

The above choice of the Gaussian range parameters is found to be suitable for describing the dilute  $N\alpha$  states.

The nuclear rms radius measured from the center-of-mass coordinate in the  $N\alpha$  state, is expressed as,

$$\sqrt{\langle r_N^2 \rangle} = \sqrt{\langle r_\alpha^2 \rangle_{HW} + 1.71^2}, \quad (26)$$

$$\langle r_\alpha^2 \rangle_{HW} = \langle \Phi_J^{(int)}(N\alpha) | \frac{1}{N} \sum_{i=1}^N (\mathbf{r}_i - \mathbf{R}_{cm})^2 | \Phi_J^{(int)}(N\alpha) \rangle, \quad (27)$$

where we take into account the finite size effect of the  $\alpha$  particle. The rms distance between two  $\alpha$  particles is given as

$$\sqrt{\langle r_{\alpha\alpha}^2 \rangle} = \left\langle \frac{1}{N(N-1)} \sum_{i,j} (\mathbf{r}_i - \mathbf{r}_j)^2 \right\rangle^{1/2} = \left( \frac{2N}{N-1} \right)^{1/2} \times \sqrt{\langle r_\alpha^2 \rangle_{HW}}. \quad (28)$$

Thus, it is proportional to the rms radius of an  $\alpha$ -particle from the center-of-mass coordinate.

### C. Effective $\alpha$ - $\alpha$ potentials.

In the present paper, we use two kinds of effective potentials: the density-dependent potential and phenomenological  $2\alpha$  plus  $3\alpha$  potential. They are applied to the Gross-Pitaevskii equation and the Hill-Wheeler equation for the study of the structure of dilute  $N\alpha$  states.

#### 1. Density-dependent potential

The density dependent potential consists of the Gaussian-type  $\alpha$ - $\alpha$  potential including a density-dependent term, which is of similar form as the Gogny potential (known as an effective  $NN$  potential) used in nuclear mean-field calculations,

$$v_2(\mathbf{r}, \mathbf{r}') = v_0 \exp[-0.7^2(\mathbf{r} - \mathbf{r}')^2] - 130 \exp[-0.475^2(\mathbf{r} - \mathbf{r}')^2] \\ + (4\pi)^2 g \delta(\mathbf{r} - \mathbf{r}') \rho \left( \frac{\mathbf{r} + \mathbf{r}'}{2} \right) + v_{Coul}(\mathbf{r}, \mathbf{r}'), \quad (29)$$

where the units of  $v_2$  and  $r$  are MeV and fm, respectively, and  $\rho$  denotes the density of the  $N\alpha$  system. The folded Coulomb potential  $v_{Coul}$  is presented as

$$v_{Coul}(\mathbf{r}, \mathbf{r}') = \frac{4e^2}{|\mathbf{r} - \mathbf{r}'|} \text{erf}(a|\mathbf{r} - \mathbf{r}'|). \quad (30)$$



The Gaussian-potential part in Eq. (29) is based on the Ali-Bodmer potential [14], which is known to reproduce well the elastic  $\alpha$ - $\alpha$  scattering phase shift up to about 60 MeV for  $v_0 = 500$  MeV. On the contrary, here, the two parameters,  $v_0$  and  $g$ , are chosen so as to reproduce well the experimental energy ( $E_3^{exp}=0.38$  MeV) and the calculated rms radius (4.29 fm by Tohsaki et al. [10]) for the  $0_2^+$  state of  $^{12}\text{C}$  by solving the Gross-Pitaevskii equation in Eq. (4). The results are  $v_0=271$  MeV and  $g=1650$  MeV $\cdot$ fm<sup>6</sup>, where the calculated energy and rms radius for the  $3\alpha$  system are 0.38 MeV and 4.14 fm, respectively, which are discussed in Sec. III. Although the choice of the phenomenological potential in Eq. (29) is rather rough, it is interesting to study systematically the structure of the  $N\alpha$  condensate states as a function of  $N$ .

## 2. Phenomenological $2\alpha$ and $3\alpha$ potential

There are many phenomenological  $2\alpha$  potentials proposed so far. Since the  $\alpha$  particle is treated as a point-like boson in the present study, we will use a  $2\alpha$  potential taking into account the Pauli blocking effect. The typical potential is the Ali-Bodmer one [14], which is used frequently in the structure calculation;  $v_2(\mathbf{r}, \mathbf{r}') = 500 \exp[-0.7^2(\mathbf{r} - \mathbf{r}')^2] - 130 \exp[-0.475^2(\mathbf{r} - \mathbf{r}')^2] + v_{Coul}(\mathbf{r}, \mathbf{r}')$ , where  $v_{Coul}$  denotes the folded Coulomb potential given in Eq. (30). The strong repulsion in the inner region prevents the  $2\alpha$  particles from approaching one another. It is, however, found that the potential is not suitable to describe the property of the compact shell-model-like structure of the  $^{12}\text{C}$  ground state with the  $3\alpha$  boson model [15]. However, we may use it for the dilute  $N\alpha$  states. The Ali-Bodmer potential, however, has the following three unfavorable properties for the present calculation.

First is that the potential does not give the experimental resonant energy of the  $^8\text{Be}$  ground state ( $E_{2\alpha}^{cal}=68$  keV vs.  $E_{2\alpha}^{exp}=92$  keV ), although the  $\alpha$ - $\alpha$  scattering phase shift is reproduced nicely up to about 60 MeV. The second is that applying the potential to the  $3\alpha$  boson system the lowest energy state obtained corresponds to a relatively compact  $3\alpha$ -structure state, although the condensate state appears around the  $3\alpha$  threshold. According to the stochastic variational calculation [16], for example, the calculated energy and rms radius are, respectively,  $E_{3\alpha}^{cal} = -0.62$  MeV and  $\sqrt{\langle r_N^2 \rangle}=3.15$  fm [17]. The results indicate that the Ali-Bodmer potential is not adequate for describing the dilute  $3\alpha$ -boson state of  $^{12}\text{C}$ . The third unfavorable point comes from the fact that the strong repulsive character in

the short-range region of the Ali-Bodmer potential ( $\sim 400$  MeV) leads us to treat exactly the short-range correlation between the  $2\alpha$  bosons. The treatment is difficult and needs time-consuming numerical calculations for solving general  $N\alpha$ -boson systems, even if employing modern numerical methods for many body systems.

We construct here an effective  $2\alpha$  potential with a weak repulsive part (soft core), which overcomes the above-mentioned three unfavorable properties. The use of such a soft-core-type  $2\alpha$  potential is suitable in the present study, because we discuss the gas-like  $N\alpha$  states, where the Pauli blocking effect between two  $\alpha$  particles is considerably weakened. The important point for the determination of the potential parameters, other than the condition of reproducing the experimental resonant energy for the  ${}^8\text{Be}$  ground state, is that the  $\alpha$ - $\alpha$  wave function for the resonant state, should have a loosely-bound structure of the two  $\alpha$  particles. According to many structure calculations of  ${}^8\text{Be}$ , the amplitude of the radial part of the  $\alpha$ - $\alpha$  relative wave function must be small in the inner region and have a maximum value around  $r = 4$  fm (where  $\mathbf{r}$  is the relative coordinate between the two  $\alpha$  particles). This condition ensures that the ground state of  ${}^8\text{Be}$  has a dilute  $2\alpha$  structure. With a careful search of the potential parameters, we determined the effective  $2\alpha$  potential as follows,

$$v_2(\mathbf{r}, \mathbf{r}') = 50 \exp \left[ -0.4^2(\mathbf{r} - \mathbf{r}')^2 \right] - 34.101 \exp \left[ -0.3^2(\mathbf{r} - \mathbf{r}')^2 \right] + v_{Coul}(\mathbf{r}, \mathbf{r}'), \quad (31)$$

where the units of  $v_2$  and  $r$  are MeV and fm, respectively, and  $v_{Coul}$  is the folded Coulomb potential. The calculated resonant energy of  ${}^8\text{Be}$  is  $E_{2\alpha}=92$  keV, in agreement with the experimental data ( $E_{2\alpha}^{exp}=92$  keV). Figure 1 shows the radial part of the relative wave function between the  $2\alpha$  clusters for the resonant state. We see that the amplitude is relatively small for  $r = 0 \sim 2$  fm, and has a maximum value around  $r=4$  fm. In spite of the fact that the Ali-Bodmer potential gives a wave function which is almost zero for  $r = 0 \sim 1$  fm, the small but finite amplitude around  $r = 0 \sim 2$  fm should hardly give any effect for dilute multi  $\alpha$  cluster states. Applying this effective potential to the  $3\alpha$ - and  $4\alpha$ -boson systems indicates that we get the desired dilute  $3\alpha$ - and  $4\alpha$ -structure states for  ${}^{12}\text{C}$  and  ${}^{16}\text{O}$ , respectively, within our framework, as shown below.

In the present study, we introduce the phenomenological  $3\alpha$  potential ( $v_3$ ) with repulsive character, as given in Ref. [18],

$$v_3(\mathbf{r}, \mathbf{r}', \mathbf{r}'') = 151.5 \exp \left\{ -0.15 \left[ (\mathbf{r} - \mathbf{r}')^2 + (\mathbf{r}' - \mathbf{r}'')^2 + (\mathbf{r}'' - \mathbf{r})^2 \right] \right\}, \quad (32)$$

where the units of  $v_3$  and  $r$  are MeV and fm, respectively. This potential has been used in the  $3\alpha$  and  $4\alpha$  orthogonally condition model (OCM [19]) for calculations of  $^{12}\text{C}$  and  $^{16}\text{O}$  so as to reproduce the ground-state energies with respect to the  $3\alpha$  and  $4\alpha$  thresholds, respectively [18]. In the model, the Pauli principle is taken into account in the relative wave function between two  $\alpha$  particles, and a deep attractive potential is used for the  $\alpha$ - $\alpha$  potential. Thus, the OCM is able to describe not only the shell-model-like compact states but also the dilute gas-like states. According to the results, the repulsive  $3\alpha$  potential gives a large effect to the ground-state energies of  $^{12}\text{C}$  and  $^{16}\text{O}$  with the compact  $N\alpha$  structure, while its effect is very small for dilute  $3\alpha$  and  $4\alpha$  states. A non-negligible effect, however, can be expected in large-number  $N\alpha$  dilute systems, if we take into account the fact that the contribution of the binding energy from the  $3\alpha$  potential, proportional to  $N(N-1)(N-2)/6$ , raises strongly with increasing  $N$ .

The reason of why we introduce the repulsive  $3\alpha$  potential is given as follows. Let us define here the total kinetic energy and two-body potential energy in the dilute  $N\alpha$  system as  $\langle T \rangle$  and  $\langle V_2 \rangle$ , respectively. In case of the  $^8\text{Be}$  ground state, the experimental energy is  $E = \langle T \rangle + \langle V_2 \rangle \sim 0.1$  MeV with respect to the  $2\alpha$  threshold, where  $\langle T \rangle$  ( $\langle V_2 \rangle$ ) is positive (negative). For an arbitrary dilute  $N\alpha$ -boson system, the total kinetic energy and two-body potential energy are given as  $\langle T \rangle \sim N - 1$  and  $\langle V_2 \rangle \sim N(N - 1)/2$ , respectively, where the center-of-mass kinetic energy is subtracted. Increasing the number of the  $\alpha$  particles, therefore, the potential energy prevails over the kinetic energy, and then, the system falls gradually into a collapsed state. This indicates that something like a density-dependent force with the repulsive character is needed to avoid the collapse in the large-number  $N\alpha$ -boson system. The present repulsive  $3\alpha$  potential in Eq. (32) plays a role similar to the density-dependent force. On the other hand, the density-dependent potential given in Eq. (29) is also used when solving the Gross-Pitaevskii equation and the Hill-Wheeler equation. The reason of why the density-dependent potential is introduced there is the same as that discussed here.

### III. RESULTS AND DISCUSSION

#### A. Application of the Gross-Pitaevskii equation to $N\alpha$ systems

The Gross-Pitaevskii equation is solved with the two different types of effective  $\alpha$ - $\alpha$  potentials: 1) the density-dependent potential [see Eq. (29)] and 2) the phenomenological  $2\alpha$  potential with the  $3\alpha$  potential [see Eqs. (31) and (32)]. First of all, we will discuss the results with the density-dependent potential and then those with the phenomenological potentials.

The calculated total energies of the  $N\alpha$  systems measured from the  $N\alpha$  threshold are demonstrated in Fig. 2 as well as the calculated nuclear rms radii defined in Eq. (11), where the density-dependent  $\alpha$ - $\alpha$  potential is used. The total energy and the rms radius are getting larger with increasing  $N$ . This means that the system is expanding steadily with increase of  $N$ . In comparison with the rms radius of the ground state of each nucleus with the empirical formula ( $\sqrt{\langle r_N^2 \rangle} = 1.2A^{1/3}$  fm), the results from the Gross-Pitaevskii equation are much larger than those for the ground states. Thus, the states obtained here can be identified with the dilute  $N\alpha$  states. It is noted that they are obtained naturally from the Gross-Pitaevskii equation with the density-dependent  $\alpha$ - $\alpha$  potential, whose parameters were determined so as to reproduce well the experimental energy ( $E_{3\alpha}^{exp}=0.38$  MeV) and the calculated rms radius by Tohsaki et al. (4.29 fm) [10] for the  $0_2^+$  state of  $^{12}\text{C}$ .

In order to study the structure of the dilute  $N\alpha$  states, it is instructive to see the single  $\alpha$  potential defined in Eq. (5). Figures 3(a)~(j) show the ones for the  $3\alpha \sim 11\alpha$  systems. Let us first discuss the  $3\alpha$  and  $4\alpha$  cases. The remarkable characteristics of the potentials can be presented as follows: 1) the almost flat behavior of the potential in the inside region, and 2) the Coulomb potential barrier in the outer region. The appearance of the flat potential region is very impressive, if one takes into account the fact that the two-range Gaussian term (attractive), density-dependent term (repulsive) and the Coulomb-potential term (repulsive) contribute significantly to the single  $\alpha$  potential in the inside region [see Figs. 3(a) and (b)]. Table I shows the calculated single  $\alpha$  particle energy and contributions from the kinetic energy, two-range Gaussian term in Eq. (29), density-dependent term in Eq. (29) and the Coulomb potential. It is found that the kinetic energy in the  $3\alpha$  and  $4\alpha$  systems is not negligible but small in comparison with the two-range-Gaussian term and/or

Coulomb potential energy. This indicates that the Thomas-Fermi approximation, neglecting the kinetic energy term, is roughly realized in the system. Consequently, there appears the flat potential region in the single  $\alpha$  potential, whose behavior is similar to the dilute atomic condensate state trapped by the magnetic fields at very low temperature [7]. On the other hand, the appearance of the Coulomb potential barrier plays an important role in confining the  $\alpha$  bosons in the inside region. It is noted that the barrier comes out naturally from the self-consistent calculation of the Gross-Pitaevskii equation. The single  $\alpha$  particle energy for the  $3\alpha$  and  $4\alpha$  systems are smaller than the Coulomb potential barrier. This means that the dilute states are quasi-stable against  $\alpha$  decay.

Increasing the number of  $\alpha$  bosons beyond  $N = 5$ , the following interesting features can be seen in the single  $\alpha$  particle potentials: 1) the depth of the flat potential becomes shallower, and its range is expanding to the outer region faster than  $\propto N^{1/3}$ , and 2) the height of the Coulomb potential barrier is getting lower and almost disappears at around  $N = 10$ . The first behavior of the potentials means that the  $N\alpha$  system is inflating with increase of  $N$ , as inferred from the behavior of the rms radius shown in Fig. 2. The reason of why the depth of the potential becomes shallower is related to the fact that the single  $\alpha$  particle energy is getting larger. It is given as follows: From Table I, the contribution from the kinetic energy to the single  $\alpha$  particle energy becomes smaller with increase of  $N$ , reflecting the inflation of the dilute  $N\alpha$  system. This fact indicates that the Thomas-Fermi approximation is getting better, and then, the single  $\alpha$  particle energy is given approximately as the contribution from only the potential energies. The potential energies consist of three contributions, namely, the two-range Gaussian term, density-dependent term, and Coulomb potential [see Eq. (29)], where the first and second ones are short-range, and the third is long-range. When the dilute  $N\alpha$  system is inflating with  $N$  and the distance between two  $\alpha$  bosons is getting larger, the contribution from the long-range potential should overcome steadily the one from the short-range one. Consequently, the potential depth (single  $\alpha$  particle energy) becomes gradually shallower (larger) and the height of the Coulomb barrier is getting lower, with increase of  $N$ . The increase of the single  $\alpha$  particle energy means that the total energy of the dilute  $N\alpha$  system becomes larger with  $N$ . The present results are consistent with the behavior of the  $N$  dependence of the total energy (see Fig. 2).

The second interesting behavior of the single  $\alpha$  particle potential with  $N \geq 5$  is that there exists a critical number of  $\alpha$  bosons,  $N_{cr}$ , beyond which the system is not confined anymore,

as mentioned in Sec. I. Around  $N = 10$ , the Coulomb barrier has almost disappeared, and the single  $\alpha$  particle potential is nearly flat up to the outer region, although the most outer region, dominated by only the Coulomb potential, is falling to zero (not illustrated in Fig. 3). Thus, we can roughly estimate the critical number as  $N_{cr} \sim 10$ , namely,  $^{40}\text{Ca}$ .

It is interesting to compare the above results with those obtained by using the Gross-Pitaevskii approach with the phenomenological  $2\alpha$  and  $3\alpha$  potentials given in Eqs. (31) and (32), respectively. The calculated total energies and rms radii for  $N\alpha$  systems are shown in Fig. 4. We find that they are in good agreement with those of the case with the density-dependent potential in the Gross-Pitaevskii equation within about 10% except for the  $N = 3$  and 4 cases. Table II shows the single  $\alpha$  particle energies and contributions from the kinetic energy and potential energies. Comparing them with those in Table I, the  $N$  dependence of the kinetic energy, Coulomb potential energy and the sum of other potential energies is rather similar to the one with the density-dependent potential in the Gross-Pitaevskii equation except for the  $N = 3$  and 4 systems. This is surprising if taking into account the fact that the forms of the two kinds of the effective  $\alpha$ - $\alpha$  potentials are quite different from one to another. These results might indicate that the dilute  $N\alpha$  systems with  $N \geq 5$  do not depend strongly on the details of the effective  $\alpha$ - $\alpha$  potential, while those with a small-number- $N\alpha$  ( $N = 3$  and 4) are sensitive to the potential.

The single  $\alpha$  particle potentials are shown in Fig. 5. For the  $3\alpha$  and  $4\alpha$  systems, we see the almost flat potential behavior in the inside region, and the Coulomb potential barrier in the outer region, while increasing the number of  $\alpha$  bosons from  $N = 5$ , the depth of the flat potential becomes shallower, and its range is expanding to the outer region, and the height of the Coulomb potential barrier is getting lower and almost disappears at around  $N = 10$ . The qualitative potential behaviors are almost the same as those in case of the density-dependent potential with the Gross-Pitaevskii equation (see Fig. 3). In fact, the behavior of the single  $\alpha$  particle potential in Fig. 5 is in good agreement with that in Fig. 3 within about 10%. On the other hand, we can conjecture the critical number  $N_{cr}$  from the behavior of the single  $\alpha$  potentials in Fig. 5, which is estimated roughly as  $N_{cr} \sim 10$ , the result being the same as that of the case with the density-dependent potential.

## B. $N\alpha$ systems in the Hill-Wheeler-equation approach

The Gross-Pitaevskii equation is simple and useful for the study of the structure of the dilute  $N\alpha$  system, as seen in the previous subsection. The center-of-mass motion in the  $N\alpha$  system, however, is not completely removed in this framework. The Hill-Wheeler-equation approach is free from the center-of-mass motion of the  $N\alpha$  system. The effect of the center-of-mass motion is expected to be non-negligible for the total energy and rms radius etc. in small-number  $\alpha$ -boson systems, in particular,  $N = 3$  and 4. Thus, it is important to study the dilute  $N\alpha$  systems with the use of the Hill-Wheeler equation. The two approaches should give the same results for dilute  $N\alpha$  systems with rather large number of  $N$ . In this subsection, we first demonstrate that the Hill-Wheeler-equation approach is useful to describe the dilute  $N\alpha$  states with the spherical shape, and the results are briefly compared with those from the Gross-Pitaevskii equation. Then, the approach is applied to the deformed  $N\alpha$  systems ( $J^\pi = 0^+$ ) with axial symmetry. We use the phenomenological  $2\alpha$  and  $3\alpha$  potentials of Eqs. (31) and (32) as the effective  $\alpha\alpha$  potential.

### 1. Spherical $N\alpha$ systems

The calculated total energies and rms radii for spherical  $N\alpha$  states are illustrated in Fig. 6, in which we show those obtained by solving the Gross-Pitaevskii equation with the same effective  $\alpha$ - $\alpha$  potential for comparison. We found that the calculated total energies in the Hill-Wheeler approach are almost the same as those in the Gross-Pitaevskii approach. This indicates that the center-of-mass kinetic energy correction in Eq. (4) is a very good approximation to remove the effect in the total energy. The non-negligible deviation between the two frameworks, however, can be seen in the rms radii, in particular, we have about 20 % deviation for the  $3\alpha$  system, although that is getting smaller with increasing  $N$  and it is almost zero in the  $7\alpha \sim 9\alpha$  systems (the discrepancy in the  $10\alpha$  and  $11\alpha$  systems will be discussed later). The results tell us that the center-of-mass correction for the rms radius in the Gross-Pitaevskii-equation approach [see Eqs. (11) and (12)] is not very good for the  $3\alpha$  and  $4\alpha$  systems, while it is relatively good for the  $N\alpha \geq 5\alpha$  systems, and the difference between the two approaches is less than about 10 %, and it is diminishing with increasing  $N$ .

In Fig. 6 we see that the deviation of the rms radius appears again in the  $10\alpha$  and  $11\alpha$  systems. The reason of why this deviation occurs can be understood, recalling the following facts: According to the results of the Gross-Pitaevskii equation with the phenomenological  $2\alpha$  and  $3\alpha$  potentials, the  $10\alpha$  system is the critical one which can not exist as a nuclear state, as mentioned in the previous section. In such a critical system, the behavior of the wave functions in the outer (inner) region is very sensitive (not very sensitive) to how to solve the equations and to obtain the wavefunctions. The value of the rms radius (total energy) is generally sensitive (not very sensitive) to the behavior of the wave function in the outer region. Thus, the re-occurrence of the deviation in the rms radii indicates that the  $10\alpha$  system is critical in the Hill-Wheeler-equation approach.

The above results show us that the Hill-Wheeler-equation approach is very useful to describe the dilute  $N\alpha$  states as well as the Gross-Pitaevskii-equation approach. Thus, we can apply the approach to the deformed  $N\alpha$  system with the axial deformation.

## 2. Deformed $N\alpha$ systems with $J^\pi = 0^+$

The  $N\alpha$  states ( $J^\pi = 0^+$ ) with the axial deformation are obtained by solving the Hill-Wheeler equation in Eq. (23) with the Gaussian size parameter set A given in Table III. Figure 7 illustrates the calculated energies, nuclear rms radii defined in Eq. (11) and the rms distances between  $2\alpha$  bosons. The detailed values are shown in Table IV. The rms distance between  $2\alpha$  bosons ( $6 \sim 11$  fm) for  $N = 3 \sim 12$  is considerably larger than that of the  $^8\text{Be}$  ground state ( $\sim 4$  fm). The result indicates that the  $N\alpha$  states obtained here are of very dilute  $N\alpha$  structure.

The total energy of the  $N\alpha$  state increases gradually with  $N$ , although those for  $N=3$  and 4 are not changed very much. The latter is in contrast to the results of the spherical case together with those for the Gross-Pitaevskii-equation approach (see Figs. 2, 4 and 6). In the  $3\alpha$  and  $4\alpha$  systems, the total energies and nuclear rms radii are respectively given as follows;  $E = -0.01$  and  $0.13$  MeV, and  $\sqrt{\langle r_N^2 \rangle} = 3.73$  and  $3.90$  fm. The values are in good correspondence to those for the condensate  $\alpha$  cluster states discussed by Tohsaki et al. [10], where their calculated results are  $E^{cal} = 0.5$  and  $-0.7$  MeV (vs.  $E^{exp} = 0.38$  and  $-0.44$  MeV) and  $\sqrt{\langle r_N^2 \rangle} = 4.29$  and  $3.97$  fm, respectively, for the dilute  $3\alpha$  and  $4\alpha$  states. It is instructive here to compare the present results with those in the spherical  $N\alpha$  states in order to estimate



the effect of deformation. The comparison of the total energy and rms radius is given in Table IV. The energy gains (reductions of rms radius) due to the deformation in the  $3\alpha$ ,  $4\alpha$  and  $5\alpha$  systems are, respectively, 0.6, 1.5 and 1.7 MeV (11 %, 18 % and 19 %), while this is getting smaller for  $N \geq 6$ . Thus, we found that the deformation effect is significant for relatively small-number  $\alpha$  systems, and shows a good correspondence of our results for the  $3\alpha$  and  $4\alpha$  states with those by Tohsaki et al. [10]. The present result that the dilute  $N\alpha$  states ( $J^\pi = 0^+$ ) may be deformed is natural if taking into account the fact that a gas-like  $N\alpha$  state with relatively small number can easily be deformed. If it is right, there may exist dilute  $N\alpha$  nuclear states with  $J^\pi = 2^+$  and  $4^+$  etc. In fact, a candidate of the dilute  $3\alpha$  state with  $J^\pi = 2^+$  is observed at  $E=3.3$  MeV measured from the  $3\alpha$  threshold [20]. The dilute multi  $\alpha$  cluster states with non-zero angular momentum will be discussed elsewhere.

From Fig. 7(a), we notice that the gas-like  $N\alpha$  states with  $N \geq 5$  appear above the  $N\alpha$  threshold, not close to it, in contrast to the fact that the dilute  $3\alpha$  and  $4\alpha$  states are located in the vicinity of their respective thresholds. This is a non-trivial result of the present calculation. The reason of why the energy of the dilute  $N\alpha$  states increases with  $N$  is given as follows. Let us consider the effective energy of the "2 $\alpha$ " system in the dilute  $N\alpha$  state, which corresponds to the quantity of the total energy of the  $N\alpha$  state divided by the number of  $\alpha$  pairs which is given in Table IV. Since the dilute character allows us to neglect approximately the kinetic energy, the effective energy of the "2 $\alpha$ " system could be given mainly as the sum of the  $2\alpha$  nuclear potential energy and its Coulomb potential energy (the contribution from the  $3\alpha$  potential may be neglected approximately because of the very small amount). Figure 8 shows the  $2\alpha$  potential used in the present study, where we also show the  $2\alpha$  nuclear potential [see Eq. (31)] and its Coulomb potential [see Eq. (30)]. The attraction of the former is largest around 4 fm and is negligible beyond about 7 fm, while the Coulomb potential is long-ranged and its repulsion is substantial even beyond 7 fm. Increasing the number of the  $\alpha$  particles, the gas-like  $N\alpha$  system is expanding and the rms distance between two  $\alpha$  particles is also becoming larger (6  $\sim$  10 fm) in the case of  $N \geq 5$ , as shown in Fig. 7. Then, the attractive contribution from the  $2\alpha$  nuclear potential to the effective "2 $\alpha$ " energy should become noticeably smaller with increasing  $N$ , reflecting the short-range (attractive) behavior of the potential. The repulsive contribution from the Coulomb potential, however, should not be much smaller than in the case of the  $2\alpha$  nuclear potential, and dominate over the contribution from the nuclear potential, because of the

long-range (repulsive) behavior. These facts explain the raise of the effective "2 $\alpha$ " energy with  $N$ , which means that the energy of the dilute  $N\alpha$  states increases with  $N$  and does not stay around the threshold energy. In Table IV we can find quantitatively the increase of the effective 2 $\alpha$  system with  $N$ . The gradual dominance of the total Coulomb potential energy over the total 2 $\alpha$  nuclear potential energy in the  $N\alpha$  system can be also seen in Table IV.

It is interesting to see the role of the 3 $\alpha$  potentials in the dilute  $N\alpha$  system. From Table IV, the contribution to the total energy is small in the case of  $^{12}\text{C}$  and  $^{16}\text{O}$ , while it gives a non-negligible effect with increasing  $N$ , as seen in Table III, because it is proportional to the number of  $N(N-1)(N-2)/6$ . In fact, the energy  $\langle V_3 \rangle$  becomes steadily larger with the number of  $\alpha$  bosons, although the quantity of the energy divided by the number of trios of the  $\alpha$  bosons is decreasing with  $N$ , reflecting the fact that the  $N\alpha$  system is expanding with  $N$ . It is instructive to study the case of no 3 $\alpha$  potentials within the present framework. The calculated results show that the  $N\alpha$  system gradually falls into a collapsed state with increasing  $N$  as discussed before; for example,  $E \sim -55$  MeV and  $\sqrt{\langle r_N^2 \rangle} = 4.77$  fm for  $N = 40$ . The result tells us that the dilute  $\alpha$  boson states appear under the cooperative work between the two-body and three-body potentials in the present model.

Finally, we estimate the critical number  $N_{cr}$  of the dilute  $N\alpha$  state beyond which the system is unbound. Since the critical state should be very unstable, it is difficult to determine it exactly with the present Hill-Wheeler-equation approach. However, we can deduce it approximately from studying the stability of the calculated eigen energies and rms radii against changing the model space determined by the Gaussian size parameters in Eqs. (24) and (25). The procedure is as follows. The present framework is able to describe dilute states trapped by the Coulomb barrier under the condition that we choose the range of the Gaussian size parameters wide enough to cover a configuration space over the whole rms radius of the states. If the state is stable or relatively stable, the calculated energies and rms radii are not changed very much against the variation of the Gaussian size parameters. Otherwise, those depend sensitively on the choice of the parameters. Using the wide model space, however, a special attention must be paid to investigate the eigen-states obtained from the Hill-Wheeler equation, because a discretized continuum state, which is unphysical, has a chance to become the lowest state in energy in the present variational calculation. We can easily identify it by investigating the behavior of its energy and/or rms radius against changing the Gaussian size parameters. The unphysical state usually has an abnormally

long rms radius, which is a little smaller than or almost the same as the value of  $b_1^{(k_{max})}$  or  $b_3^{(K_{max})}$  in Eqs. (24) and (25). Table V shows the calculated results for the two parameter sets A and B (see Table III). The calculated energies and rms radii for the dilute  $N\alpha$  states with  $N = 3 \sim 10$  are almost the same for both the parameter sets A and B, while we see some discrepancies in those with  $N \geq 11$ , in particular, in the rms radii, for the two parameter sets. Even if we use other Gaussian size parameter sets which cover the configuration space over the rms radius for the dilute states, the results obtained are found to be similar to those mentioned above. Thus, the critical number of the dilute  $N\alpha$  boson systems is estimated roughly to be  $N_{cr} \sim 10$ , namely,  $^{40}\text{Ca}$ , in the present study. It is noted that the number is the same as that in the spherical case as well as in the Gross-Pitaevskii-equation approach.

#### IV. SUMMARY

The dilute  $N\alpha$  cluster condensate states with  $J^\pi = 0^+$  have been studied with the Gross-Pitaevskii equation (GP) and the Hill-Wheeler equation (HW), where the  $\alpha$  cluster is treated as a structureless boson. Two kinds of effective  $\alpha$ - $\alpha$  potentials were used: the density-dependent  $\alpha$ - $\alpha$  potential (DD) and the phenomenological  $2\alpha$  potential plus 3-body  $\alpha$  potential (PP), and we also included the folded Coulomb potential between the  $2\alpha$  bosons. Both potentials (only the latter) were (was) applied to study the structure of the spherical (spherical and axially deformed) dilute  $N\alpha$  states with the Gross-Pitaevskii equation (Hill-Wheeler equation). Thus, we have studied the dilute multi  $\alpha$  cluster states with the four different frameworks; (equation, potential, shape)=(GP, DD, S), (GP, PP, S), (HW, PP, S) and (HW, PP, D), where S and D denotes the spherical and deformed shapes, respectively.

The main results to be emphasized here are as follows:

- 1) All of the  $N\alpha$  states obtained show the dilute  $N\alpha$  structure. They are common to all of the four different frameworks. The reason of why the total energy of the gas-like  $N\alpha$  state increases gradually with  $N$  and do not remain around their  $N\alpha$  threshold values is understood as the competition between the nuclear  $\alpha$ - $\alpha$  nuclear potential (attractive) and its Coulomb potential (repulsive). In fact, increasing the number of  $N$ , the  $\alpha$ - $\alpha$  distance is becoming larger (6  $\sim$  12 fm for  $N = 3 \sim 12$ ), and then the contribution from the  $\alpha$ - $\alpha$  nuclear potential per  $2\alpha$  pair in the dilute  $N\alpha$  state is decreasing rapidly because of the short-range character, while that from the Coulomb one is decreasing very slowly and remains almost

constant for  $N = 5 \sim 12$ , reflecting the  $1/r$  character of the Coulomb potential.

2) The  $N$  dependence of the behavior of the calculated single  $\alpha$  potentials obtained by solving the Gross-Pitaevskii equation within the (GS, DD, S) and (GW, PP, S) frameworks is impressive. For the  $3\alpha$  and  $4\alpha$  systems, we see an almost flat potential behavior in the inside region, and the Coulomb potential barrier in the outer region, while increasing the number of  $\alpha$  bosons from  $N = 5$ , the depth of the flat potential becomes shallower, and its range is expanding to the outer region, while the height of the Coulomb potential barrier is decreasing and almost disappears at around  $N = 10$ . The origin of the appearance of the flat region is mainly due to the validity of the Thomas-Fermi approximation, namely, the neglect of the contribution from kinetic energy because of the dilute character of the  $N\alpha$  system. The result is analogous to the dilute atomic condensate state trapped by the magnetic fields at very low temperature. On the other hand, the results for the total energy and rms radius were quite similar for the above-mentioned two frameworks except for  $N=3$  and 4. The result might indicate that the dilute  $N\alpha$  states with  $N \geq 5$  are not very sensitive to the details of the effective  $\alpha$ - $\alpha$  potential (DD or PP).

3) Comparing the results from the Gross-Pitaevskii equation (GP) and Hill-Wheeler equation (HW), we could see the effect of the neglect of the center-of-mass motion in the Gross-Pitaevskii equation and also the usefulness of the Hill-Wheeler-equation approach for describing the dilute  $N\alpha$  system. In the small-number  $N\alpha$  systems, the effect was found to be non-negligible, in particular, for the rms radius, while there is less than about 10 % deviation for the  $N\alpha \geq 5\alpha$  systems.

4) The axial deformation effect in the dilute  $N\alpha$  systems is substantial for the small-number  $\alpha$  systems, but it is getting smaller for  $N \geq 6$ . In fact, the energy gain and reduction of the rms radius due to the deformation are  $0.6 \sim 1.7$  MeV and  $11 \sim 19$  %, respectively, for the former system. Due to the effect, the calculated results of the total energy and rms radius for  $N=3$  and 4 in the (HW, PP, D) framework are improved from those in the (HW, PP, S) framework, and give a good correspondence with those for the condensate  $\alpha$  cluster states discussed by Tohsaki et al. [10] The present result that the dilute  $N\alpha$  states ( $J^\pi = 0^+$ ) may be deformed is natural, taking into account the fact that a gas-like  $N\alpha$  state with relatively small number of  $\alpha$ 's could easily be deformed.

5) We estimated the critical number of the  $\alpha$  bosons,  $N_{cr}$ , beyond which the system is unbound for the four frameworks, (GP, DD, S), (GP, PP, S), (HW, PP, S) and (HW, PP, D).

All of the frameworks indicated that the number is roughly  $N_{cr} \sim 10$ , which is not strongly dependent on the frameworks. Thus, we concluded that the dilute  $N\alpha$  cluster states could exist in the  $^{12}\text{C}$  to  $^{40}\text{Ca}$  systems with  $J^\pi = 0^+$ , whose energies vary from threshold up to about 20 MeV in the present calculation.

The estimate of  $N_{cr} \sim 10$  is of course subject to the validity of our phenomenological approach treating the  $\alpha$ -particles as ideal bosons. We, however, believe, for reasons outlined in the paper, that our estimate for  $N_{cr}$  may be correct to within  $\pm 20\%$ . In any case the value for  $N_{cr}$ , *i.e.* the maximum of  $\alpha$ -particles in the condensate state is relatively modest. A very interesting question in this context is whether adding a few neutrons may stabilize the condensate and thus allow for much higher numbers of condensed  $\alpha$ 's. One should remember that  $^8\text{Be}$  is (slightly) unbound whereas  $^9\text{Be}$  and  $^{10}\text{Be}$  are bound.

Concerning experimental detection of the  $\alpha$ -condensates, the decay scheme of the dilute  $N\alpha$  state is conjectured to proceed mainly via  $\alpha$  decay. This indicates that such systems may be observed through the following sequential  $\alpha$  decays: [dilute  $N\alpha$  state]  $\rightarrow$  [dilute  $(N-1)\alpha$  state] $+\alpha$ , [dilute  $(N-1)\alpha$  state]  $\rightarrow$  [dilute  $(N-2)\alpha$  state] $+\alpha$ ,  $\dots$ . Therefore, the sequential  $\alpha$  decay measurement is expected to be one of the promising tools to search for the dilute multi- $\alpha$  cluster states, produced via the  $\alpha$  inelastic reaction, heavy-ion collision reaction, and so on. It is highly hoped to perform such the experiments in near future.

### Acknowledgments

We greatly acknowledge helpful discussions with Y. Funaki, H. Horiuchi, K. Ikeda, G. Röpke, and A. Tohsaki. One of the authors (T.Y.) is very grateful to the Theory Group of the Institut de Physique Nucléaire, Université Paris-Sud (Paris XI) for its hospitality during his sabbatical year.

- 
- [1] K. Wildermuth and Y.C. Tang, *A Unified Theory of the Nucleus* (Vieweg, Braunschweig, Germany, 1977).
- [2] D.M. Brink, in *Many-Body Description of Nuclear Structure and Reactions*, Proceedings of the International School of Physics "Enrico Fermi", Course 36, edited by C. Bloch (Academic Press, New York, 1966).
- [3] G.F. Bertsch and W. Bertozzi, Nucl. Phys. **A165**, 199 (1971).
- [4] Y. Fujiwara, H. Horiuchi, K. Ikeda, M. Kamimura, K. Kato, Y. Suzuki, and E. Uegaki, Prog. Theor. Phys. Suppl. No. 68, 29 (1980).
- [5] K. Ikeda, N. Takigawa, and H. Horiuchi, Prog. Theor. Phys. Suppl. Extra Number, 464 (1968).
- [6] For example, H. Horiuchi and K. Ikeda, *Cluster Model of the Nucleus*, International Review of Nuclear Physics, World Scientific Publishing Co., **4**, 1 (1986).
- [7] F. Dalfovo, S. Giorgini, L.P. Pitaevskii, and S. Stringari, Rev. Mod. Phys. **71**, 463 (1999).
- [8] G. Röpke, A. Schnell, P. Schuck, and P. Noziers, Phys. Rev. Lett. **80**, 3177 (1998).
- [9] M. Beyer, S.A. Sofianos, C. Kuhrts, G. Röpke, and P. Schuck, Phys. Lett. B **80**, 247 (2000).
- [10] A. Tohsaki, H. Horiuchi, P. Schuck and G. Röpke, Phys. Rev. Lett. **87**, 192501 (2001).
- [11] Y. Funaki, H. Horiuchi, A. Tohsaki, P. Schuck and G. Röpke, Prog. Theor. Phys. **108**, 297 (2002).
- [12] L.P. Pitaevskii, Zh. Eksp. Theor. Fiz. **40**, 646 (1961) [Sov. Phys. JETP **13**, 451 (1961)]; E.P. Gross, Nuovo Cimento **20**, 454 (1961); J. Math. Phys. **4**, 195 (1963).
- [13] D.L. Hill and J.A. Wheeler, Phys. Rev. **89**, 1102 (1953).  
J.J. Griffin and J.A. Wheeler, Phys. Rev. **108**, 311 (1957).
- [14] S. Ali and A.R. Bodmer, Nucl. Phys. **80**, 99 (1966).
- [15] R. Tamagaki and Y. Fujiwara, Prog. Theor. Phys. Suppl. No. 61, 229 (1977).
- [16] Y. Suzuki and M. Takahashi, Phys. Rev. C **65**, 064318 (2002).
- [17] In Ref. [16], the calculated value is 2.64 fm, which is not taken into account the finite size effect of the  $\alpha$  particle. With help of the Eq. (26) in this paper, the nuclear rms radius  $\sqrt{\langle r_N^2 \rangle}$  is 3.15 fm.
- [18] K. Fukatsu and K. Kato, Prog. Theor. Phys. **87**, 151 (1992).
- [19] S. Saito, Prog. Theor. Phys. **40** (1968) 893; **41**, 705 (1969).

[20] F. Ajzenberg-Selove, Nucl. Phys. A506, 1 (1990).

TABLE I: Calculated results of the Gross-Pitaevskii equation with the density-dependent  $\alpha$ - $\alpha$  potential in Eq. (29); single  $\alpha$  particle energy  $\varepsilon$  and contributions from the kinetic energy  $\langle t \rangle$ , two-range-Gaussian term  $\langle v_{2G} \rangle$ , density-dependent term  $\langle v_D \rangle$  and Coulomb potential  $\langle v_C \rangle$  in Eq. (29). The total energy and nuclear rms radius for the  $N\alpha$  system are denoted as  $E$  and  $\sqrt{\langle r_N^2 \rangle}$ , respectively. All energies and rms radii are given, respectively, in units of MeV and fm.

$N$	nucleus	$\varepsilon$	$\langle t \rangle$	$\langle v_{2G} \rangle$	$\langle v_C \rangle$	$\langle v_D \rangle$	$E$	$\sqrt{\langle r_N^2 \rangle}$
3	$^{12}\text{C}$	0.18	0.38	-3.42	2.31	0.91	0.38	4.14
4	$^{16}\text{O}$	0.78	0.32	-3.74	3.04	1.16	1.44	4.91
5	$^{20}\text{Ne}$	1.32	0.28	-3.90	3.69	1.25	2.97	5.53
6	$^{24}\text{Mg}$	1.82	0.25	-3.95	4.25	1.26	4.94	6.07
7	$^{28}\text{Si}$	2.28	0.22	-3.91	4.76	1.21	7.36	6.58
8	$^{32}\text{S}$	2.72	0.20	-3.80	5.20	1.20	10.2	7.05
9	$^{36}\text{Ar}$	3.13	0.19	-3.65	5.59	1.00	13.4	7.51
10	$^{40}\text{Ca}$	3.51	0.18	-3.45	5.93	0.86	17.0	7.98
11	$^{44}\text{Ti}$	3.87	0.18	-3.19	6.19	0.69	21.0	8.46



TABLE II: Calculated results of the Gross-Pitaevskii equation with the phenomenological  $2\alpha$  and  $3\alpha$  potentials in Eqs. (31) and (32); single  $\alpha$  particle energy  $\varepsilon$  and contributions from the kinetic energy  $\langle t \rangle$ ,  $2\alpha$  potential  $\langle v_2 \rangle$  in Eq. (31),  $3\alpha$  potential  $\langle v_3 \rangle$  in Eq. (32) and Coulomb potential  $\langle v_C \rangle$ . The total energy and nuclear rms radius for the  $N\alpha$  system are denoted as  $E$  and  $\sqrt{\langle r_N^2 \rangle}$ , respectively. All energies and rms radii are given, respectively, in units of MeV and fm.

$N$	nucleus	$\varepsilon$	$\langle t \rangle$	$\langle v_2 \rangle$	$\langle v_C \rangle$	$\langle v_3 \rangle$	$E$	$\sqrt{\langle r_N^2 \rangle}$
3	$^{12}\text{C}$	0.45	0.25	-1.90	1.96	0.14	0.98	4.87
4	$^{16}\text{O}$	0.76	0.27	-2.71	2.86	0.33	1.84	5.23
5	$^{20}\text{Ne}$	1.12	0.27	-3.36	3.68	0.53	3.04	5.55
6	$^{24}\text{Mg}$	1.51	0.26	-3.89	4.44	0.70	4.63	5.85
7	$^{28}\text{Si}$	1.91	0.26	-4.31	5.13	0.84	6.61	6.13
8	$^{32}\text{S}$	2.31	0.24	-4.64	5.78	0.94	8.99	6.40
9	$^{36}\text{Ar}$	2.73	0.23	-4.89	5.37	1.02	11.8	6.68
10	$^{40}\text{Ca}$	3.13	0.22	-5.06	6.91	1.60	15.0	6.95
11	$^{44}\text{Ti}$	3.53	0.20	-5.15	7.40	1.70	18.6	7.24

TABLE III: Gaussian size parameter sets A and B used to obtain the deformed  $N\alpha$  states with the axial symmetry by solving the Hill-Wheeler equation. The unit of  $b_1$  and  $b_3$  is fm.

set	$k_{max}$	$b_1^{(1)}$	$b_1^{(k_{max})}$	$K_{max}$	$b_3^{(1)}$	$b_3^{(K_{max})}$
A	12	0.4	9.0	12	0.5	9.5
B	12	0.4	11.0	12	0.5	10.5

TABLE IV: Calculated total energy  $E$ , total kinetic energy  $\langle T \rangle$ , total  $2\alpha$  nuclear potential energy  $\langle V_2 \rangle$ , total Coulomb potential energy  $\langle V_C \rangle$ , total  $3\alpha$  potential energy  $\langle V_3 \rangle$  and nuclear rms radius  $\sqrt{\langle r_N^2 \rangle}$  for each dilute  $N\alpha$  state. The effective energy of the "2 $\alpha$ " system in the  $N\alpha$  system is denoted as  $\varepsilon_2$  (see text). All energies and rms radii are given in units of MeV and fm, respectively.

$N$	nucleus	deformed case							spherical case	
		$\langle T \rangle$	$\langle V_2 \rangle$	$\langle V_C \rangle$	$\langle V_3 \rangle$	$E$	$(\varepsilon_2)$	$\sqrt{\langle r_N^2 \rangle}$	$E$	$\sqrt{\langle r_N^2 \rangle}$
3	$^{12}\text{C}$	2.24	-5.95	3.62	0.09	-0.01	(-0.00)	3.73	0.64	4.18
4	$^{16}\text{O}$	3.74	-11.31	7.21	0.42	0.11	(0.02)	3.90	1.58	4.74
5	$^{20}\text{Ne}$	4.32	-15.92	11.58	1.13	1.11	(0.11)	4.20	2.83	5.19
6	$^{24}\text{Mg}$	3.71	-18.78	16.05	2.09	3.13	(0.21)	4.69	4.47	5.64
7	$^{28}\text{S}$	3.13	-21.03	20.58	0.09	5.58	(0.27)	5.24	6.48	5.99
8	$^{32}\text{Si}$	2.77	-23.16	25.31	0.09	8.30	(0.30)	5.79	8.93	6.33
9	$^{36}\text{Ar}$	2.52	-25.11	30.22	0.09	11.31	(0.31)	6.34	11.81	6.90
10	$^{40}\text{Ca}$	2.35	-26.76	35.21	0.09	14.62	(0.32)	6.90	14.98	7.26
11	$^{44}\text{Ti}$	2.26	-28.52	40.58	0.09	18.27	(0.33)	7.38	18.53	7.54
12	$^{48}\text{Cr}$	2.21	-30.43	46.37	0.09	22.63	(0.34)	7.78	22.44	8.62

TABLE V: Calculated energies  $E$  of dilute  $N\alpha$  states ( $J^\pi = 0^+$ ) together with the nuclear rms radii  $\sqrt{\langle r_N^2 \rangle}$  and rms distances between  $2\alpha$  bosons  $\sqrt{\langle r_{\alpha\alpha}^2 \rangle}$ , where we use the two Gaussian size parameter sets A and B, shown in Table III. The energy  $E$  is measured from the respective  $N\alpha$  threshold. The units of energy and rms radius (distance) are MeV and fm, respectively.

$N$	nucleus	$E$	set A		set B		
			$\sqrt{\langle r_N^2 \rangle}$	$\sqrt{\langle r_{\alpha\alpha}^2 \rangle}$	$E$	$\sqrt{\langle r_N^2 \rangle}$	$\sqrt{\langle r_{\alpha\alpha}^2 \rangle}$
3	$^{12}\text{C}$	-0.01	3.73	5.73	-0.01	3.72	5.72
4	$^{16}\text{O}$	0.11	3.90	5.72	0.11	3.90	5.72
5	$^{20}\text{Ne}$	1.11	4.20	6.06	1.13	4.20	6.06
6	$^{24}\text{Mg}$	3.13	4.69	6.76	3.13	4.68	6.75
7	$^{28}\text{Si}$	5.58	5.24	7.57	5.59	5.24	7.57
8	$^{32}\text{S}$	8.30	5.79	8.36	8.30	5.78	8.35
9	$^{36}\text{Ar}$	11.31	6.34	9.16	11.31	6.35	9.17
10	$^{40}\text{Ca}$	14.62	6.90	9.97	14.61	7.03	10.58
11	$^{44}\text{Ti}$	18.27	7.38	10.65	18.22	7.89	11.42
12	$^{48}\text{Cr}$	22.27	7.78	11.21	22.10	8.81	12.77

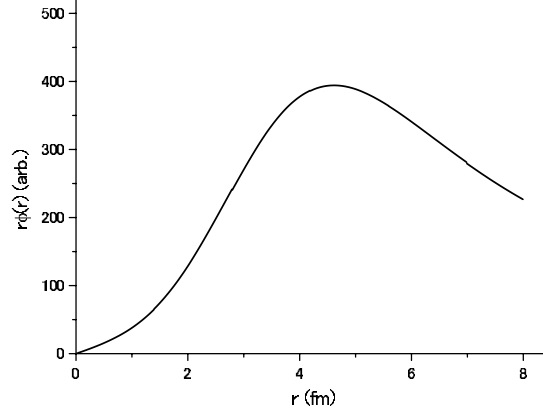


FIG. 1: Radial part of the relative wave function between the  $2\alpha$  clusters in the  $J^\pi = 0^+$  resonant state at  $E_{2\alpha}=92$  keV with use of the soft-core  $\alpha$ - $\alpha$  potential in Eq. (31). The scale of  $r\phi(r)$  is arbitrary.

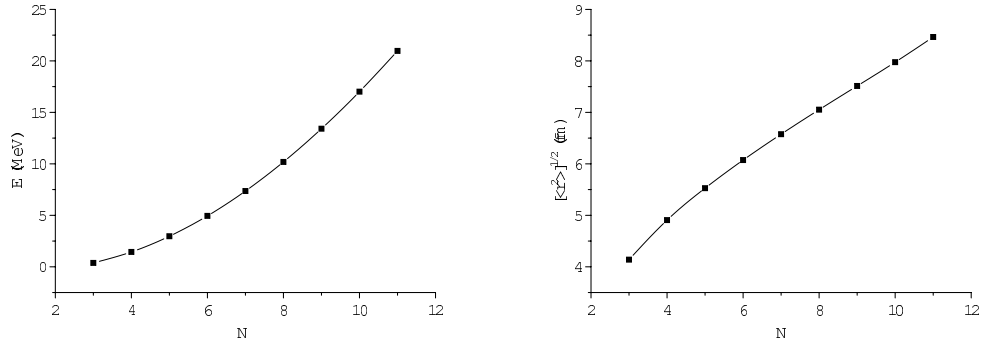
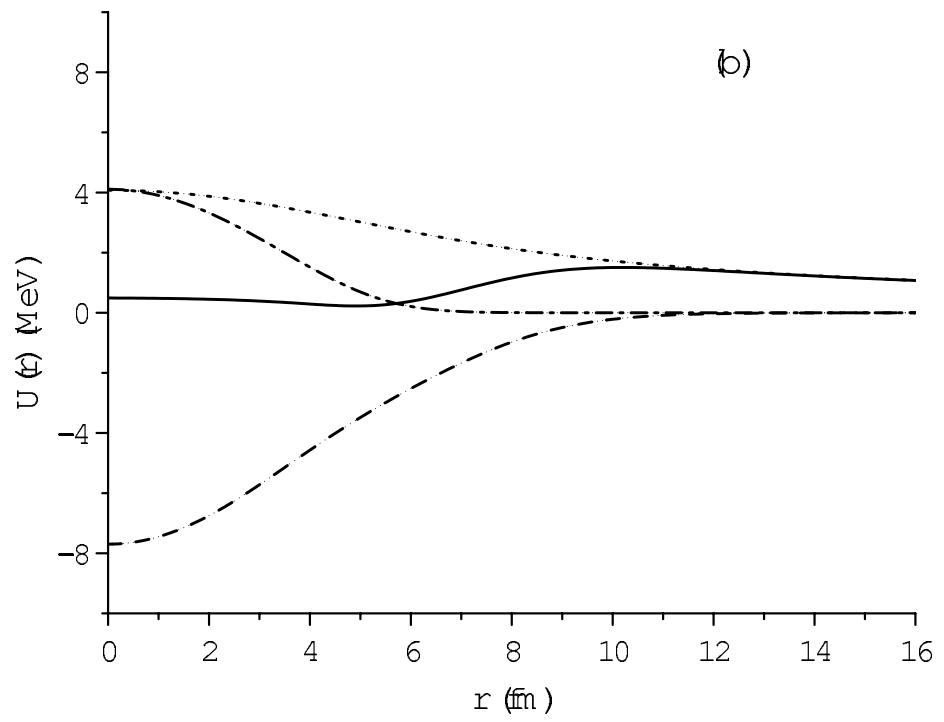
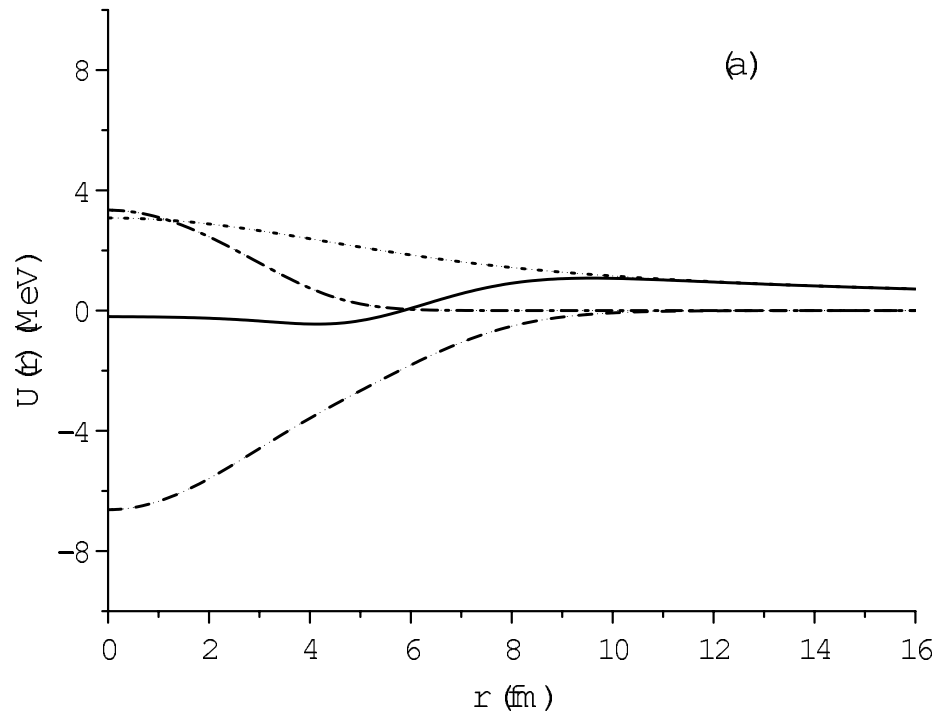
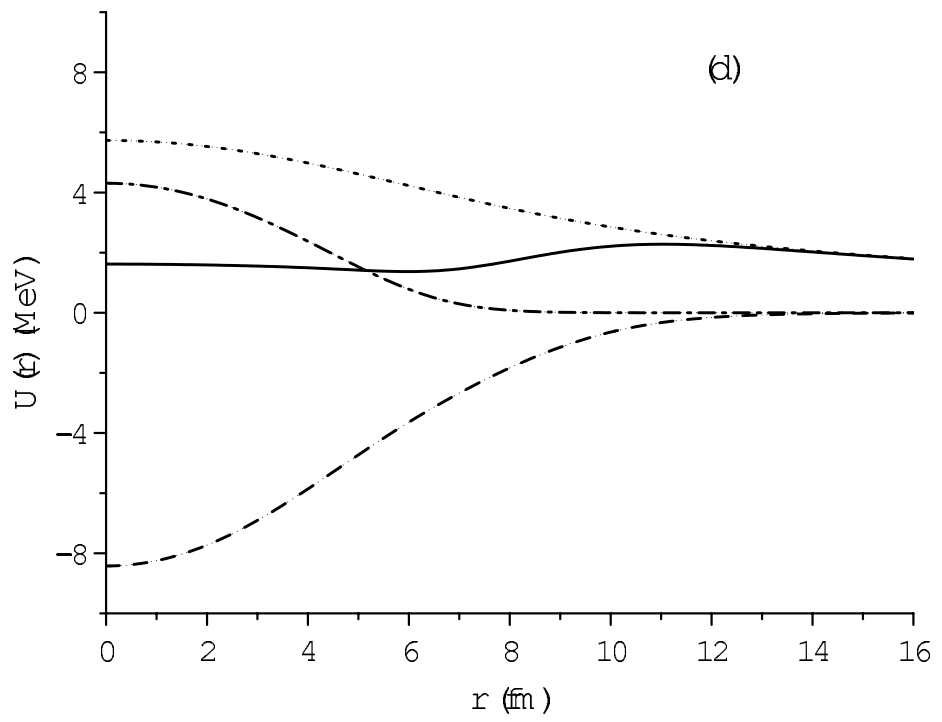
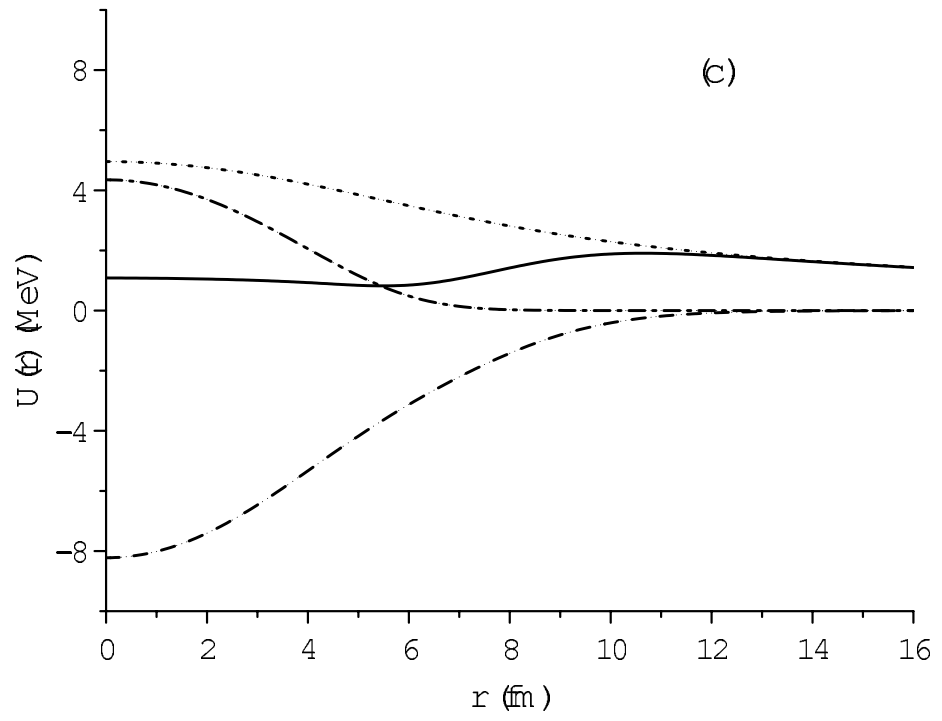
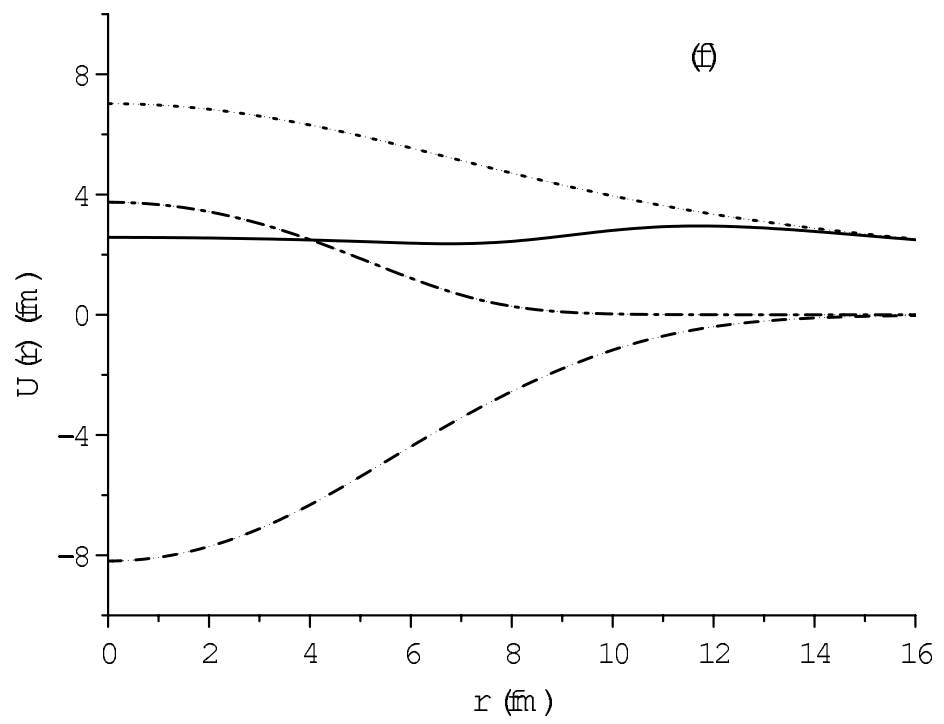
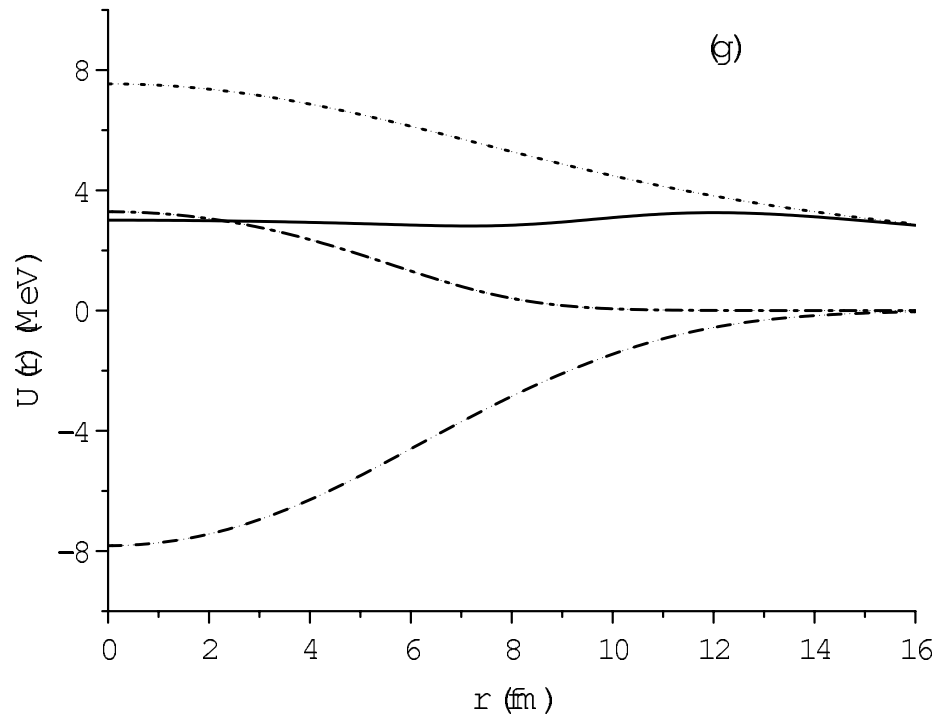


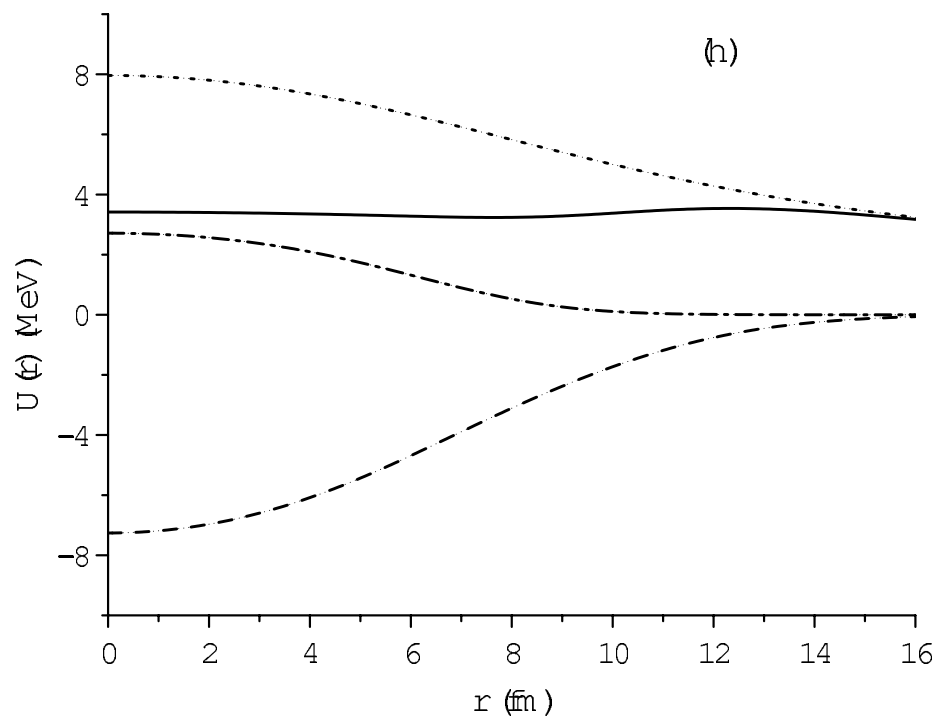
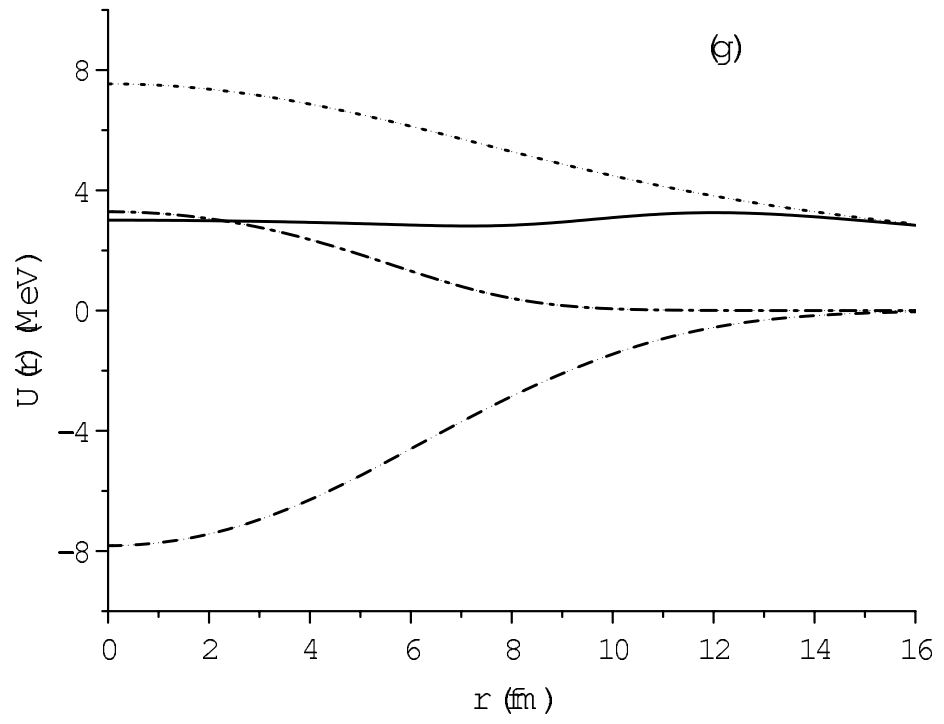
FIG. 2: (a) Total energies for the dilute  $N\alpha$  states measured from each  $N\alpha$  threshold, and (b) their nuclear rms radii, which are obtained by solving the Gross-Pitaevskii equation with the density-dependent potential.











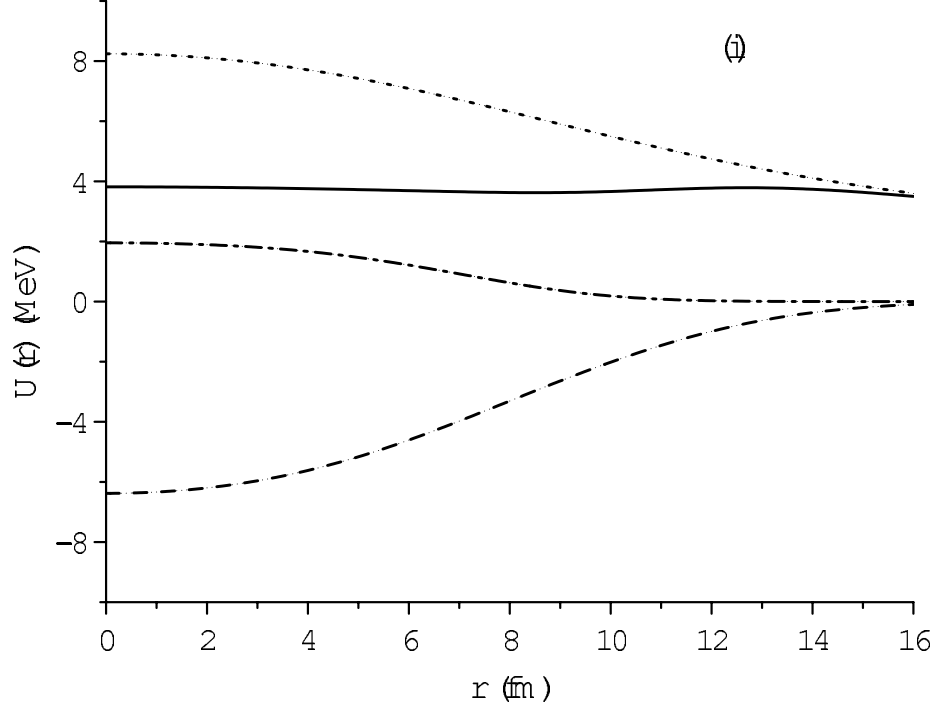


FIG. 3: Single  $\alpha$  particle potentials  $U_\alpha(R)$  (solid line) which are obtained by solving the Gross-Pitaevskii equation with the density-dependent potential; (a)  $3\alpha$ , (b)  $4\alpha$ , (c)  $5\alpha$ , (d)  $6\alpha$ , (e)  $7\alpha$ , (f)  $8\alpha$ , (g)  $9\alpha$ , (h)  $10\alpha$ , (i)  $11\alpha$  systems. The dashed, dot-dashed and dotted lines demonstrate, respectively, the contribution from the two-range Gaussian term, density-dependent term and Coulomb potential.

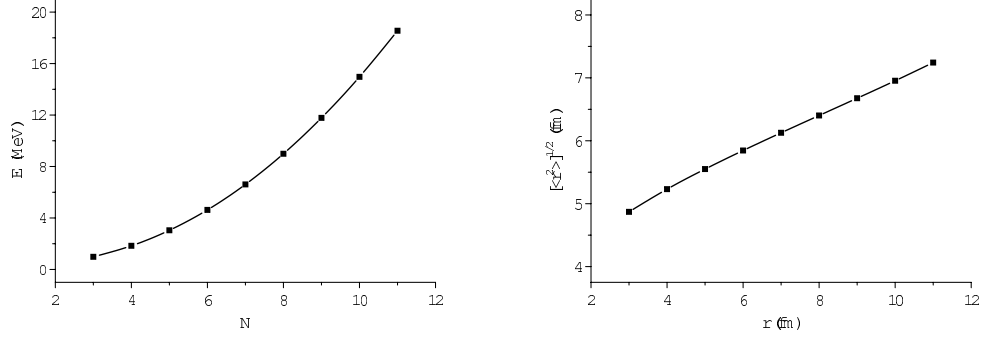
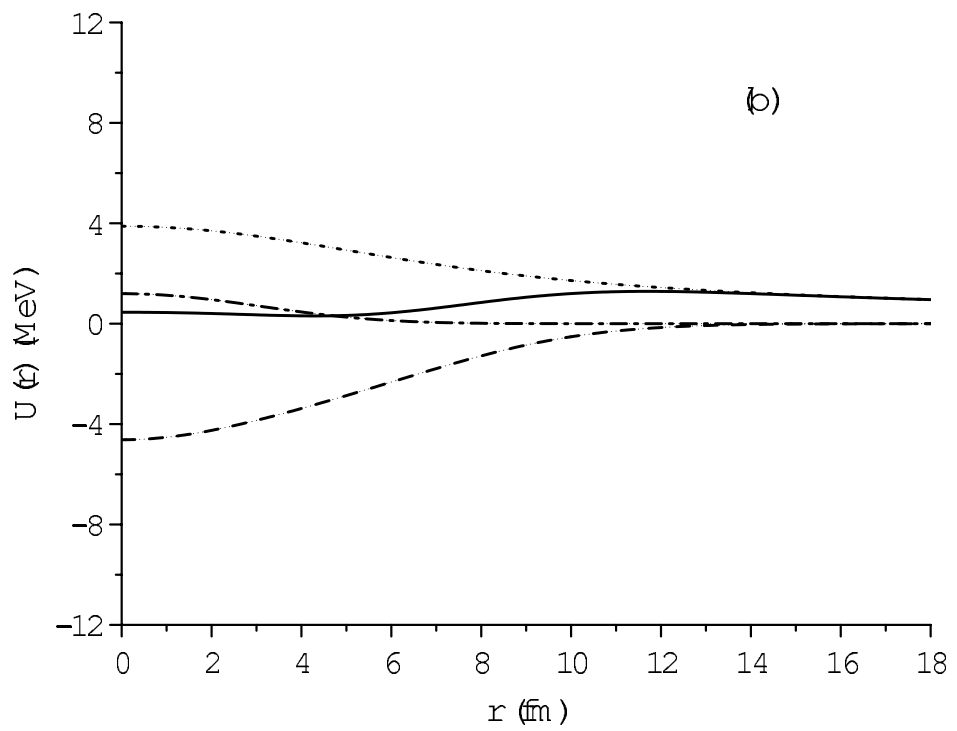
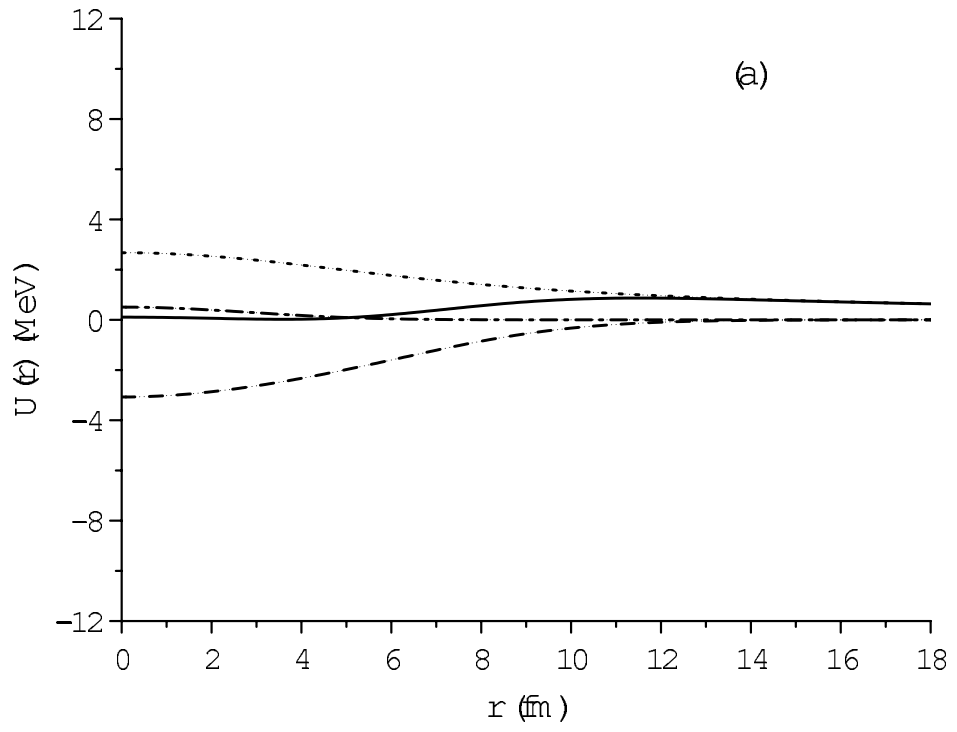
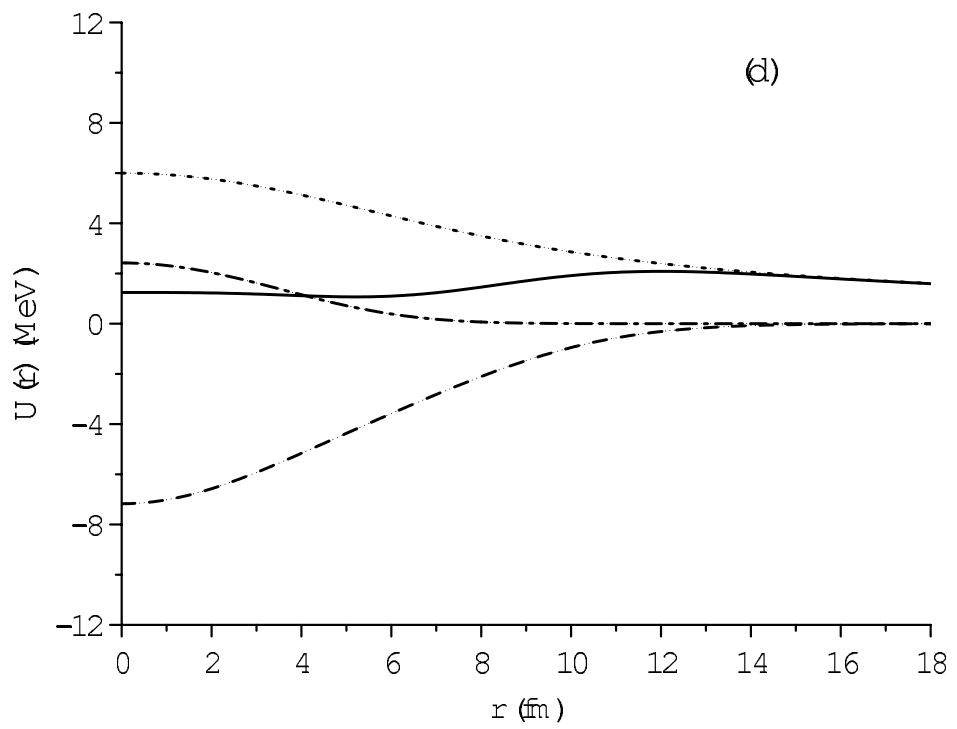
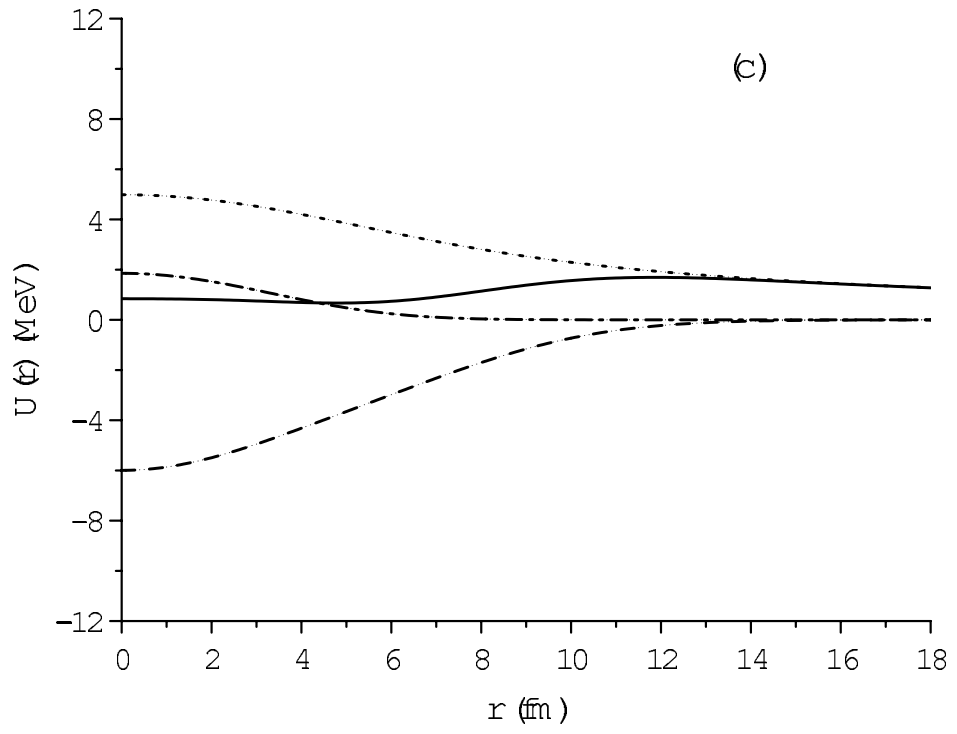
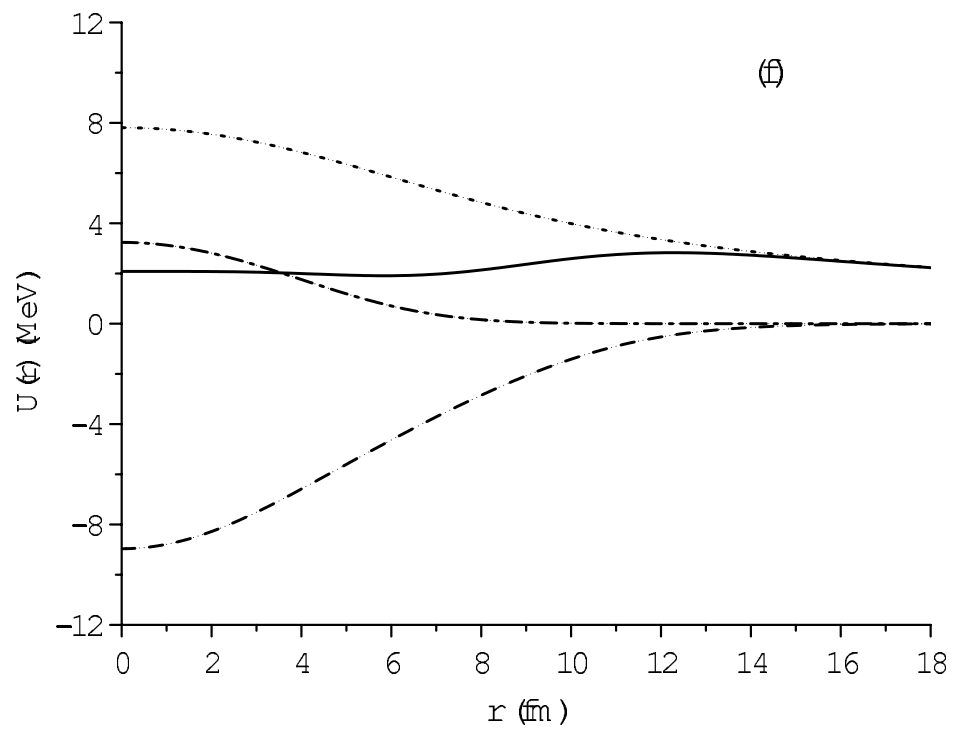
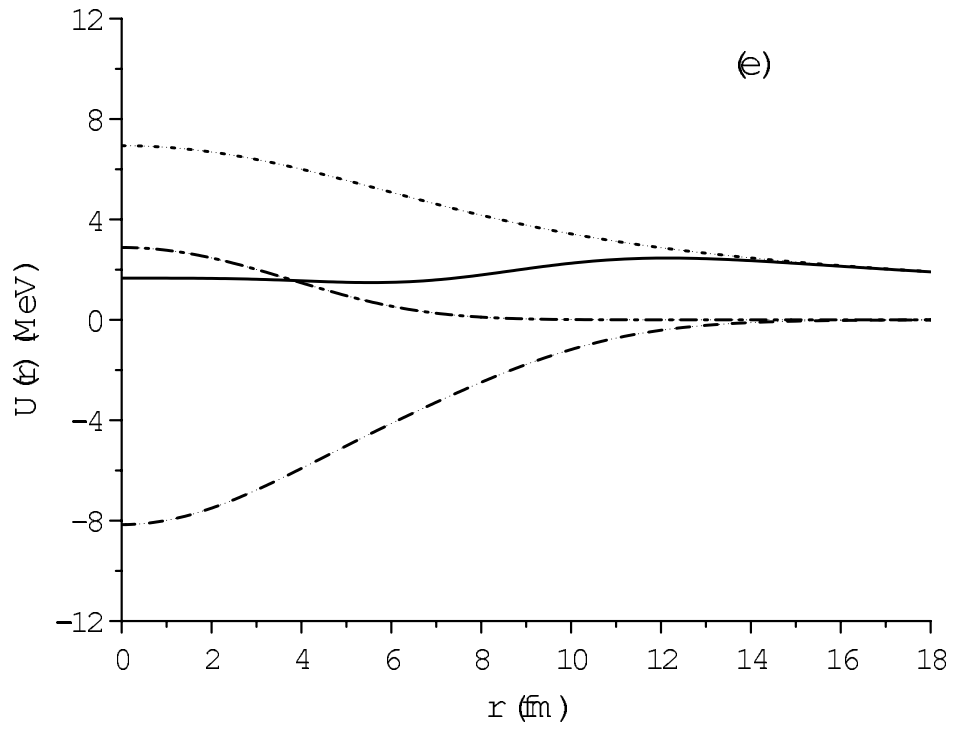
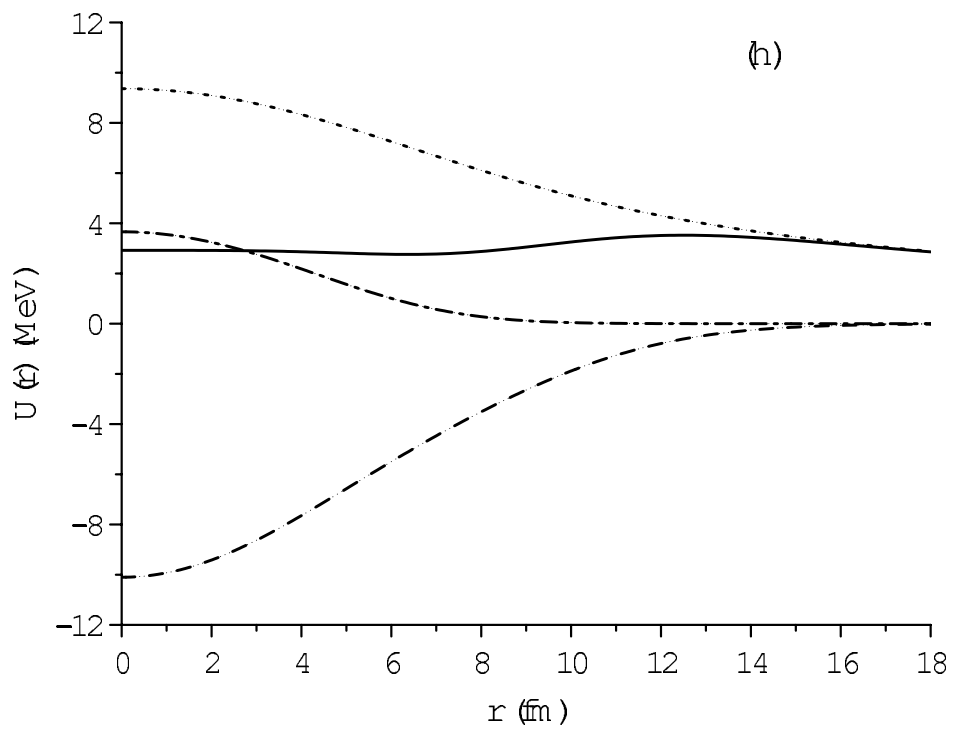
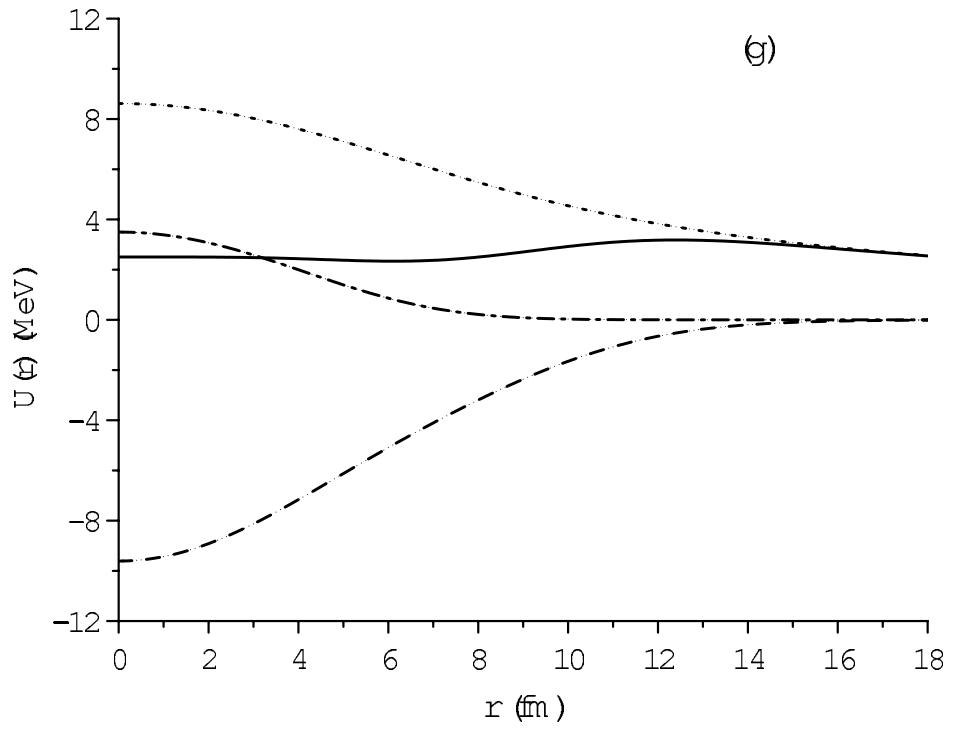


FIG. 4: (a) Total energies for the dilute  $N\alpha$  states measured from each  $N\alpha$  threshold, and (b) their nuclear rms radii, which are obtained by solving the Gross-Pitaevskii equation with the phenomenological  $2\alpha$  and  $3\alpha$  potentials.











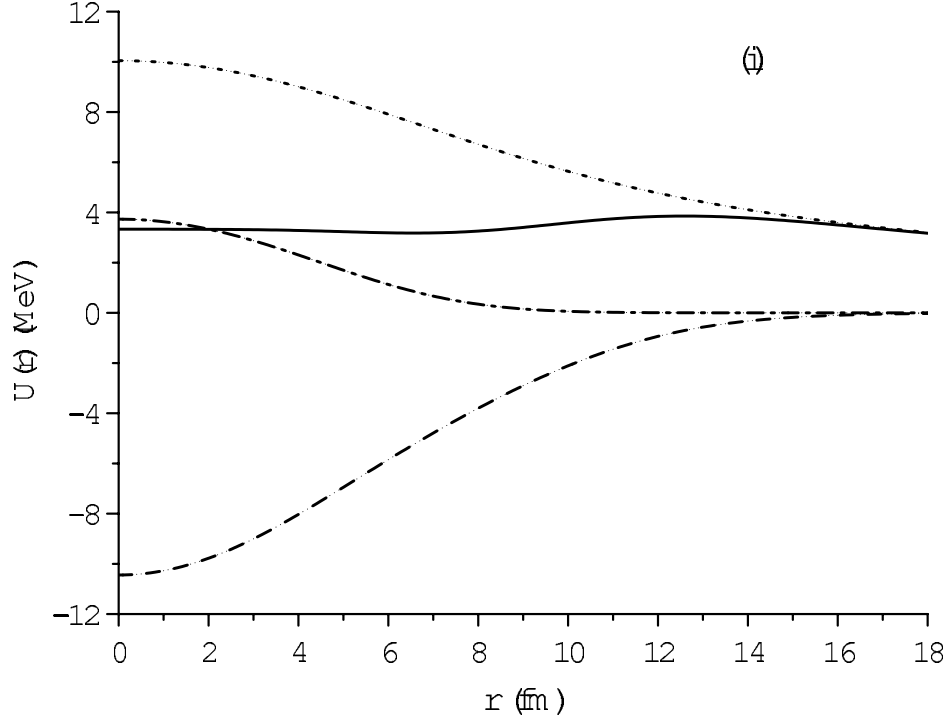


FIG. 5: Single  $\alpha$  particle potentials  $U_\alpha(R)$  (solid line) which are obtained by solving the Gross-Pitaevskii equation with the phenomenological  $2\alpha$  and  $3\alpha$  potentials; (a)  $3\alpha$ , (b)  $4\alpha$ , (c)  $5\alpha$ , (d)  $6\alpha$ , (e)  $7\alpha$ , (f)  $8\alpha$ , (g)  $9\alpha$ , (h)  $10\alpha$ , (i)  $11\alpha$  systems. The dashed, dot-dashed and dotted lines demonstrate, respectively, the contribution from the  $2\alpha$  potential,  $3\alpha$  potential and Coulomb potential.

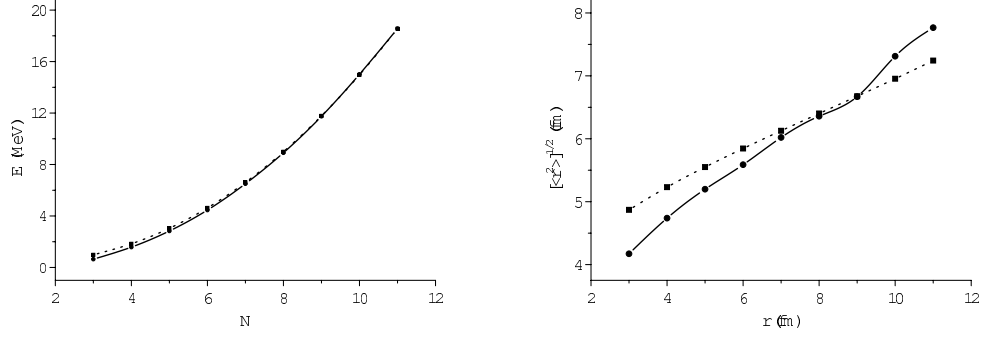


FIG. 6: (a) Total energies for the dilute  $N\alpha$  states (spherical case) measured from each  $N\alpha$  threshold (solid line), and (b) their nuclear rms radii (solid), which are obtained by solving the Hill-Wheeler equation with the phenomenological  $2\alpha$  and  $3\alpha$  potentials. For comparison, we also give the corresponding values obtained by solving the Gross-Pitaevskii equation with use of the same potentials (dotted lines).

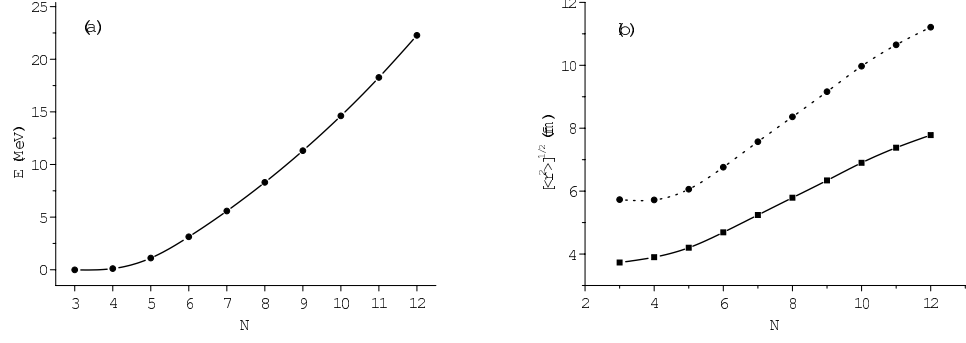


FIG. 7: (a) Total energies for the dilute  $N\alpha$  states with the axial deformation measured from each  $N\alpha$  threshold (solid line), and (b) their nuclear rms radii (solid) and rms distance between  $2\alpha$  particles (dotted), which are obtained by solving the Hill-Wheeler equation with the phenomenological  $2\alpha$  and  $3\alpha$  potentials.

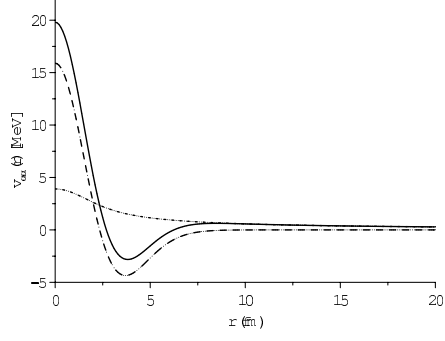


FIG. 8: Phenomenological  $2\alpha$  potential (solid line), where the  $2\alpha$  nuclear potential [Eq. (31)] and its Coulomb potential [Eq. (30)] are drawn by the dashed and dotted lines, respectively.